To the Graduate Council:

I am submitting herewith a thesis written by Daniel Lee Pfeffer entitled “Lard used as a Fuel for Hybrid Rocket Motors.” I have examined the final electronic copy of this thesis for form and content and recommend that it be accepted in partial fulfillment of the requirements for the degree of Master of Science, with a major in Aerospace Engineering.

James Evans Lyne, Major Professor

We have read this thesis
and recommend its acceptance:

Majid Keyhani

Hans Desmidt

Accepted for the Council:

Carolyn R. Hodges

Vice Provost and Dean
of the Graduate School

(Original signatures are on file with official student records.)

Lard used as a Fuel for Hybrid Rocket Motors

A Thesis Presented for
the Master of Science Degree

The University of Tennessee, Knoxville

Daniel Lee Pfeffer
May 2007

ACKNOWLEDGEMENTS

I would like to thank everyone who helped reach this goal in life. My mother and father, Margaret and Douglas Pfeffer, who have always cared for me and helped me become the person I am today. Also, I would like to thank Scott Putnam and Josh Scholes for helping me with in my research and thesis. I especially would like to thank Dr. Evans Lyne for his guidance and providing me with the opportunity to work with him on hybrid rockets. Above all I would like to thank God because without him I would have never made it. I would also like to thank Dr. Majid Keyhani and Dr. Hans DeSmidt for serving on the committee and for their teaching throughout the years. I would also like to thank Dr. Viatcheslav Naoumov for his help with the theoretical work and data analysis and Dennis Higdon for his expert help and advice in instrumentation.

ABSTRACT

A bio-derived fuel, lard, was successfully tested using a laboratory scale hybrid rocket motor and a static test stand at the University of Tennessee-Knoxville. The experimental setup used gaseous oxygen as the oxidizer. Twenty-three experimental tests were successfully conducted with lard and oxygen. The nine-inch fuel grains used in the current investigation produced a measured thrust ranging from 70-145 Newtons (15-33 pounds) with calculated specific impulses ranging from 122-181 seconds. All the tests conducted were intensely fuel rich, and had equivalence ratios ranging from 0.2 to 0.45. The low equivalence ratios are partially due to unburned fuel particles that exit the nozzle. The tests conducted have shown that the regression rate of the lard was higher than that of other fuels, such as HTPB (hydroxyl-terminated polybutadiene), used in hybrid rocket motors. Lard has produced results similar to those obtained by researchers at Stanford University using paraffin. This investigation has provided sufficient evidence to indicate that lard merits further study as a fuel for hybrid rocket motors.

Table of Contents

List of Figures

Nomenclature

a	Power curve coefficient
A_e	Exit area (m^2)
A_o	Orifice plate hole area (m^2)
$A_{p,av}$	Average port area (m^2)
A_t	Nozzle throat area (m^2)
C	Discharge coefficient
C*	Characteristic velocity (m/s)
d	Orifice plate hole diameter (m)
D	Pipe diameter (m)
D_f	Final port diameter (m)
e	Gas expansion coefficient
go	Acceleration due to gravity at the earth's surface (m/sec^2)
$G_{ox,av}$	Average oxidizer mass velocity ($kg/sec\text{-}m^2$)
G_{prop}	Average propellant mass velocity ($kg/sec\text{-} m^2$)
I	Total impulse (N-sec)
ID	Inner diameter (m)
I_{sp}	Specific impulse (sec)
K	Gas isentropic exponent
L_g	Grain length (m)
L_p	Port length (m)
m_f	Fuel mass (kg)
m_{ox}	Oxidizer fuel mass (kg)
$\dot{m}_f$	Average fuel mass flow rate (kg/sec)
$\dot{m}_{ox}$	Average oxidizer mass flow rate (kg/sec)
M_f	Burned fuel mass (kg)
M_{final}	Final Mass (kg)
$M_{initial}$	Initial mass (kg)
$\dot{m}_{ox}$	Average oxidizer mass flow rate (kg/sec)
$\dot{m}_p$	Average propellant mass flow rate (kg/sec)
M_p	Burned propellant mass (kg)
n	Power curve exponent
OD	Grain outer diameter (m)
O/F	Oxidizer to fuel ratio
$(O/F)_{stoich}$	Stoichiometric O/F value
P_a	Ambient pressure (psia)
P_c	Average combustion pressure (psig)
P_e	Exit Pressure (psig)
P_{up}	Average upstream orifice plate pressure (psig)

$\dot{r}$	Average regression rate (m/sec)
R_u	Universal gas constant (J/kmol-K)
t	Time (sec)
T	Average thrust (N)
T_c	Combustion temperature (K)
T_{ox}	Oxidizer Temperature (K)
t_b	Burn time (sec)
t_s	Case thickness (m)
u_e	Exit velocity (m/sec)
V	Volume (m^3)
β	Blowing coefficient
ΔP	Average pressure differential
δ_{gi}	Initial grain thickness (m)
δ_{gf}	Final grain thickness (m)
ϕ	Equivalence ratio
γ	Specific heat ratio
μ	Combustion gas viscosity (kg/m-s)
μ_{ox}	Molecular mass of oxidizer (kg/kmol)
μ_f	Molecular mass of fuel (kg/kmol)
ρ	Density (kg/m^3)
ρ_f	Fuel density (kg/m^3)

Chapter I
Background and Introduction

Hybrid rockets have been studied since the late 1930s. It was not, however, until the 1960s that hybrids were researched more in depth. Hybrid rockets are different from solid and liquid rockets in that hybrids use a combination of propellants in different phases. One phase is stored in a liquid or gaseous state, and the other is stored in a solid state. The most common arrangement, and the one being investigated in this study, uses a gaseous oxidizer and a solid fuel. Hybrid rockets are unique from other propulsion systems in that combustion occurs inside the boundary layer by diffusion and flow turbulence. The fuel is transported upward to the combustion zone mainly by convective heat transfer, with the oxidizer diffusing into the combustion zone. Radiation heat transfer becomes relevant only if metal particles are added to the fuel.[1] On the other hand, the propellants in solid and liquid propelled rockets are premixed before combustion occurs.

Interest in hybrid rocket motors has increased in recent years mainly because of the safety features they possess. Hybrid rocket motors are safer than solid rocket motors and liquid rocket engines because it is nearly impossible to have an explosive combination of a fuel and oxidizer. Also, the fabrication, storing, and operating are much safer since the fuel does not already have the oxidizer in intimate contact. Fuel for hybrid rockets can be made in almost any location and can be transported safely with few restrictions. Hybrids also do not have a catastrophic failure if a crack occurs in the fuel grain like in solid motors because combustion only occurs in the port where it encounters the oxygen flow.[1, 2]

Hybrid rocket systems have a number of advantages over other propulsion systems. They can be started, stopped, and restarted depending on the mission, unlike solid motors. Plus, the thrust of the rocket can be changed over a broad range during flight by varying the oxidizer flow rate. Hybrids also have a higher specific impulse than solid rocket motors and a higher density-specific impulse than bipropellant engines.[1, 2]

However, hybrid rocket motors have some setbacks that keep them from being used on a regular basis. One of the main setbacks of hybrids is their low regression rate, or the solid fuel burn rate. Most hybrid rocket research has shown significantly lower regression rates compared to solid rocket motors. Due to their low regression rates, hybrid rockets must have multiple combustion ports to generate thrust levels close to those of solid rockets using a single combustion port. However, multiple ports create a higher cost of fabrication and design. Also, multiple ports are not efficient because they increase the size of the rocket and add unnecessary mass to the rocket. Multiple ports are complex, and some ports may collapse during burning, causing large pieces of fuel to exit the nozzle unburned.

Major problems associated with current rocket propellants include the negative environmental effects and significant toxicity. Certain propellants, like hypergolic propellants, are commonly hazardous to handle and are toxic. Ammonium perchlorate (NH_4ClO_4) and oxidizers such as nitric acid (HNO_3) and fluoride (F_2) are extremely hazardous to fabricate and handle. The cost of fabricating, storing, operating, and cleanup after use of toxic fuels is extremely high. For example, ammonium perchlorate, used in solid rockets, has ended on in the ground water of hundreds of water wells in eight known states. Perchlorate has been connected with thyroid problems in humans, in which thyroid hormones govern brain development in fetuses and infants. Also, lettuce was recently discovered to be contained with the chemical because it was irrigated with contaminated ground water. The use of this chemical has cost several companies, such as GenCorp. Inc, to pay $250 million to clean up perchlorate and other toxins.[6, 7] The environmental damage not only cost these companies financially but also tarnished their reputations in the eyes of the public. Ammonium perchlorate was just one many compounds used in rockets that not only hurt the environment but also the people who live in that region. Therefore, an ideal fuel source for rockets would have a low toxicity.

Recently, hybrid rocket motors have been developed by private companies, schools, and government agencies. The best known hybrid rocket to date is SpaceShipOne, which won the X-Prize in 2004. An increasing interest in space tourism has led to a need for safer rocket travel; this, in turn, has led to more research on hybrids. Several universities, including Purdue University and the University of Alabama in Huntsville, have been conducting small scale hybrid rocket tests with different types of fuels and oxidizers. Private companies, such as Lockheed Martin and Boeing, have done large scale testing on hybrids. For example, Lockheed Martin Space Systems Michoud Operations tested a 30,000 lb thrust hybrid rocket motor at Edwards Air Force base in 2005 for 120 seconds. SpaceDev, the maker of SpaceShipOne, has completed a study that resulted in a practical concept for a safe and affordable hybrid powered human space transport system, the Dream Chaser, that would carry six passengers to and from the International Space Station.[5]

A non-toxic, environmentally friendly propellant combination that produces higher regression rates and thrust levels with a single combustion port design is needed for hybrid rocket motors to be used more frequently. Recent research by Stanford University and NASA Ames has shown that paraffin and gaseous oxygen have significantly higher regression rates compared with traditional hybrid rocket propellants. Paraffin and oxygen hybrid rockets were found to have regression rates three to four times greater than that of the previously researched combination of HTPB and oxygen.[3] The higher regression rates of paraffin are thought to result from an unstable liquid layer that forms during combustion. Droplets form on the created liquid-gas interface and increase surface area, which increases the regression rate.[1,3,4] Historically, most fuels used in hybrid rocket motors, such as HTPB, vaporized or sublimated into the combustion zone. The main difference between fuels which produce a melt layer and liquid droplets and those that vaporize is their melting points. The melting points of standard fuels are significantly higher than that of paraffin. Therefore, other solid fuels with characteristics similar to those of paraffin merit study. Thus, lard is being researched since its melting points, 40°C, is similar to that of paraffin (62°C).

In hybrid rockets, most research is done on find the regression rate equation of a fuel. There are a number of different equations used to calculate the regression rate of the fuel. Equation 1 is derived when the energy balance at the fuel grain surface is done.[1]

$$\dot{r} = 0.03\frac{G^{0.8}}{\rho_f}\left(\frac{\mu}{x}\right)^{0.2}\beta^{0.32} \qquad (1)$$

Other regression relationships are found experimentally using parameters such as the port length and the propellant and oxidizer flux rates, as shown in equations 2 and 3.[1,2]

$$\dot{r} = aG_{avg}^{n} L_{p}^{m} \tag{2}$$

$$\dot{r} = aG_{o}^{n} \tag{3}$$

where G_{avg} is average mass flux, L_p is the combustion port length, and G_o is oxidizer mass flux. The constants a and n are obtained by experimental testing. For example, a hybrid rocket that used HTPB as the fuel and oxygen as the oxidizer used equation 3 and found the constants a and n equal to 0.104 and 0.681, respectively, whereas paraffin was found to have constants a and n equal to 0.488 and 0.62, respectively.

An in depth study into the possibility of using lard and gaseous oxygen as propellants in hybrid rocket motors will be discussed in this paper. One of the primary goals of the current study was to obtain regression rate equations for lard. Regression rates were found as functions of several parameters, specifically, the oxidizer mass flux, the oxidizer mass flow rate, and the total mass propellant flow rate. These regression rate equations can be used in the future to predict engine performance and design motors for specific applications. Other parameters, such as the specific impulse (I_{sp}), equivalence ratio, combustion pressure, and thrust, were measured or calculated to evaluate the performance of the rocket.

Nitrous oxide (N_2O) was also evaluated as a potential oxidizer for lard. N_2O has been used on a number of other hybrid rockets because it is easy to obtain and relatively cheap. However, only gaseous oxygen achieved adequate results because of combustion instability with the nitrous oxide.

Chapter II explains firing procedures and the test stand apparatus. In Chapter III, results are presented and analyzed. Finally, Chapter IV discusses the conclusions from all the testing and gives suggestions for further study.

Chapter II
Experimental Setup and Procedure

2.1 Experimental Setup

Hybrid rocket testing at the University of Tennessee-Knoxville began in 2000. Over the years the experimental test stand has been improved to provide better results. A photograph and diagram of the current apparatus are shown in Figures 1-3. The test stand has been modified to withstand higher pressures and thrust. In 2006, the test stand was relocated to a more remote site due to safety considerations. At the new location, a ten foot long, six foot high, and one foot wide blast wall filled with six tons of sand was erected to protect rocket personnel during firing. The combustion assembly is taken apart and cleaned on a regular basis to avoid fuel build up in the premixing chamber. Also, flash arrestors were added to the oxidizer line to ensure that any back flash from combustion would not flow past the solenoid. A new analog to digital (A/D) converter card with a USB cable was added to move the computer away from the rocket during tests.

The fuel grain is housed in a ten inch long steel pipe that is a quarter inch thick and had an outer diameter three inches. The grain is secured in place by connecting the two steel caps with six nine sixteenths inch bolts and nuts. (see Figure 2) This is an improvement from the previous arrangement and makes the grain more secure and simplifies the changing of grains. Figure 1 shows an image of the test stand. A detailed sketch of a cross sectional view of the rocket assembly can be seen in Figure 2. The tightening of the bolt and nut assembly is extremely important during tests. The bolts must be tightened evenly and firmly or there is excessive fuel leakage when the rocket is fired. Excessive fuel leakage can cause highly inaccurate results. Leakage leads to a decrease in the thrust and combustion pressure. Also, the final mass of the fuel grain will not be correct, which affects the regression rate, if there is leakage.

Figure 1. Hybrid rocket experimental test stand setup.

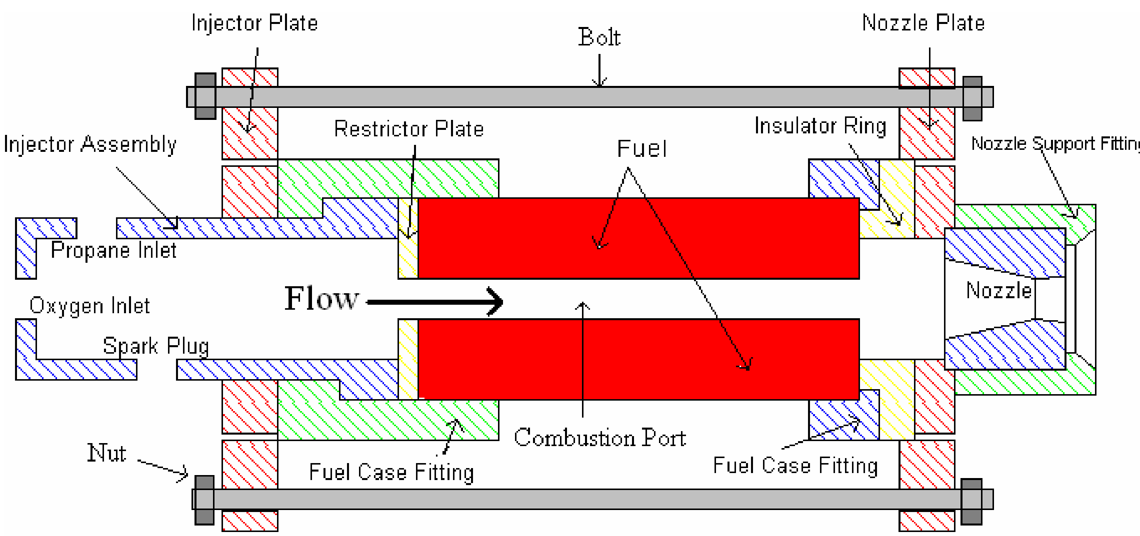

Figure 2 Cross sectional sketch of the combustion chamber

A flow chart of the entire test system can be seen in Figure 3. The system consists of an oxidizer and a propane tank flowing gas down a high pressure hose to a half inch steel pipe. A regulator is attached directly to each tank to control the supply pressure. The oxidizer supply pressure ranges from 320 to 460 psig for lard. The propane tank is set to its maximum pressure around 70 psig. A solenoid, located between the hose and the pipe, controls the flow of the gas for the desired amount of time. The oxidizer is typically set for four and half to five seconds, while the propane is set for half a second. The oxidizer gas then flows past two pressure transducers with an orifice plate between them. Next, the oxidizer and propane meet in the pre-combustion chamber and are ignited by the spark plug. Then, gases are ignited upstream of the fuel grain to initiate combustion of the fuel. A restrictor plate forces the gas to flow down the combustion port. The burned and unburned gas and fuel enter the mixing chamber and then exit through the nozzle.

2.2 Data Collection

The main objective of the experimental rocket firings was to collect accurate and reliable data regarding thrust, combustion pressure, geometry, fuel consumption and mass flow rate. Two of the main parameters, the oxygen supply and combustion pressure, were measured using two thin filmed pressure transducers (Omega PX603-1KG5V and PX613-1KG5V). An orifice between the two pressure transducers was used to calculate the oxygen mass flow rate of the rocket. The thrust was measured using a strain gauge attached to a cantilever beam near the nozzle. The strain gauge would send a signal to a strain gauge box that can adjust the signal for calibration.

All three devices (two pressure transducers and strain gauge) sent an electrical output signal into an analog to digital (A/D) converter card. The 12-bit data acquisition card (Measurement Computing MiniLAB 1008) used differential inputs and digitized the raw data from the instruments. The output signal was then transferred to the computer by a USB cable for analysis. Hewlett-Packard Visual Engineering Environment, or HP VEE, was used to collect the data.

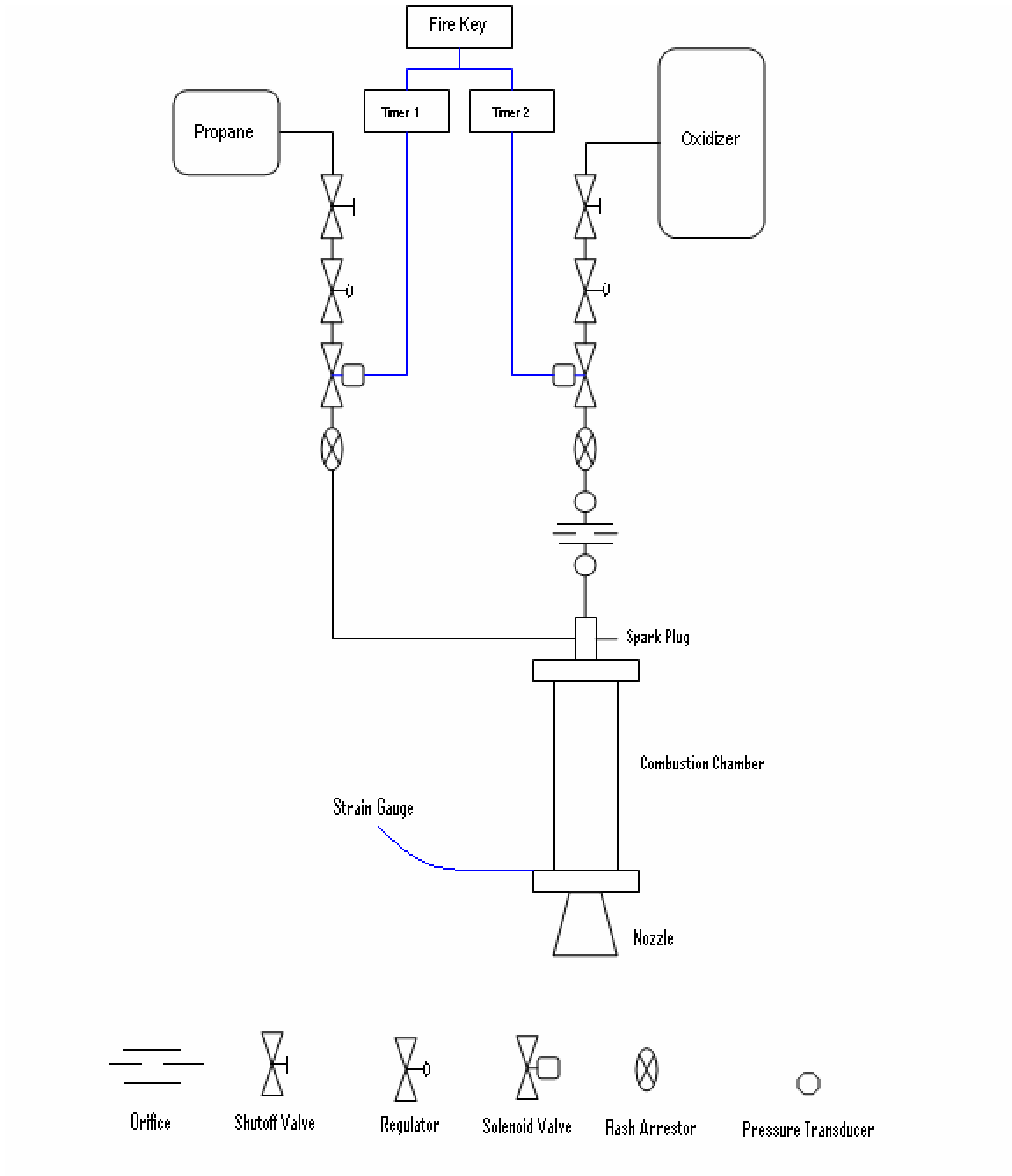

Figure 3 Flow chart for the hybrid rocket.

An HP VEE program was written to convert the output signal from each device to a useful value. The A/D card obtains readings as counts, and the HP VEE program converts the counts to a value using the parameters of the different devices. The pressure transducers and strain gauge have a voltage range of 1-5 Vdc and 0-5 Vdc, where the pressure transducers have an operational range of 0-1000 psig. The output count value of the pressure transducers was converted to psig, and the strain gauge count output was converted to volts.

To produce accurate results, a calibration of the strain gauge was done before each test. The calibration consisted of using a bucket with varying weights that covered the range of the thrust for that test. A typical calibration curve is shown in Figure 4. Using a linear approximation of the plot, the conversion equation was used to covert the voltage output to Newtons.

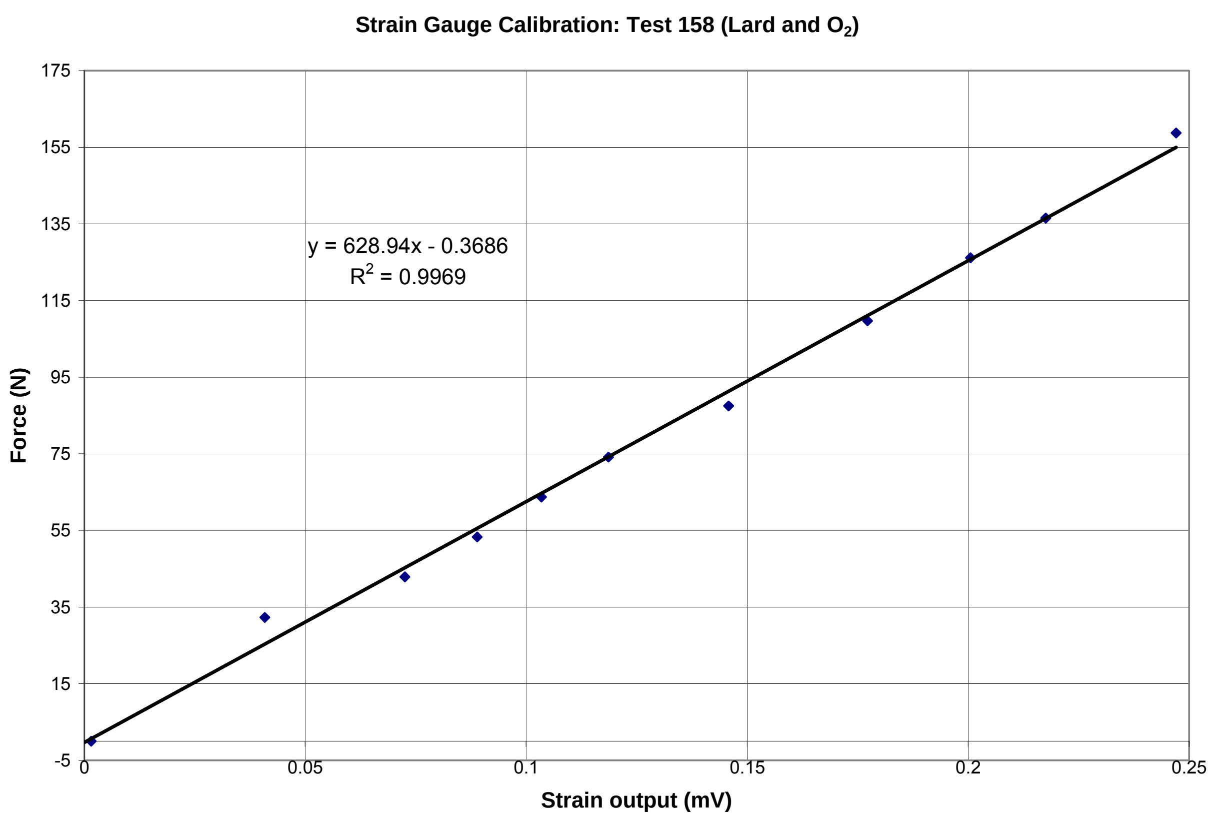

Figure 4 Strain gauge calibration for Test 158.

2.3 Grain manufacturing

Grain production was an important process for rocket testing. Grain production was started by melting the fuel (lard) to a liquid state. Lard was melted so that it can be molded into a grain. Once the fuel was liquefied, it was then poured into the sleeve. The sleeve was placed on top of a wooden base that had a cylindrical extrusion on it that created a gap for the aft mixing chamber. A polished steel rod was inserted in the center of the wooden base to create a combustion port. A problem had been occurring with the rod leaning to one side while the fuel was resolidifying on some grains. The center combustion port of the grain needed to be straight to obtain optimal results. An off-centered combustion port suppressed the oxidizer flow by partially blocking the restrictor plate's hole. Also, an uneven burn occurs where all of the fuel is burned on one side to the wall and leads to inefficient combustion. A cooper cap was placed onto the sleeve to fix this problem. The cap had a hole in the center of it for the rod to slide through and keep the rod centered. The fuel grains were then moved to a cooling location once the cap was placed on the fuel grains.

The number of tests that could be conducted depended on the number of grains available. In the beginning, only four sleeves, three rods, and four blocks were used to make grains. The insignificant amount of available grains prevented how often tests could be conducted since it takes one to two days to fully make a fuel grain. Therefore, eight new blocks, rods, and sleeves were created to produce grains at a faster rate.

The lard had to be stored in a different location because of its physical properties. Lard was moved to a freezer and had to be kept cold because it has a gelatinous state at room temperature. The lard cannot maintain a stable, solid fuel grain at room temperature. Also, the lard fuel must stay in a frozen state at the time of the rocket firing, or the grain collapses and large chunks are blown out. The fuel grains then had to be topped off after they had cooled to a solid state. Finally, the wooden base was removed and the rod was knocked out of the grain once they were cooled completely and topped off.

The quality of the grain had an effect on the outcome of the test. A grain with air bubbles in it caused an uneven burning of the grain and sometimes caused the grain to collapse. Air bubbles are believed to form when the grain has cooled off and then topped off with more fuel. If the fuel was not extremely hot when topping the grain off, then the liquid fuel did not fuse with the solid fuel and created an air gap, thus forming air bubbles. In some tests an air bubble causes a second combustion channel to form between the grain and the sleeve wall. Also, cracks have occurred while tapping the rod out.

The aft mixing chamber is an important part of the chamber design. Combustion occurs down the combustion port and then enters the aft mixing chamber. Some of the liquid fuel droplets that did not burn down the combustion port are mixed with the oxidizer by turbulent flow in the mixing chamber. Figure 5 shows a sketch of the mixing chamber in the fuel grain.

If the mixing chamber is too small, it leads to inefficient combustion because the fuel and oxidizer do not have enough time to react before exiting the nozzle. When the mixing chamber is too large it reduces the burning area and decreases the thrust. Also, an excessively large mixing chamber adds unnecessary weight to a flight vehicle. An ideal mixing chamber will have a length to diameter ratio (L/D) of 0.5 to 1.0.[2] Previous research done at the University of Tennessee had used a chamber with an L/D ratio of 0.2, which is smaller than ideal. The problem was fixed by increasing the wooden base extrusion used to form the aft mixing chamber by an inch to acquire a more ideal L/D ratio of 0.75.

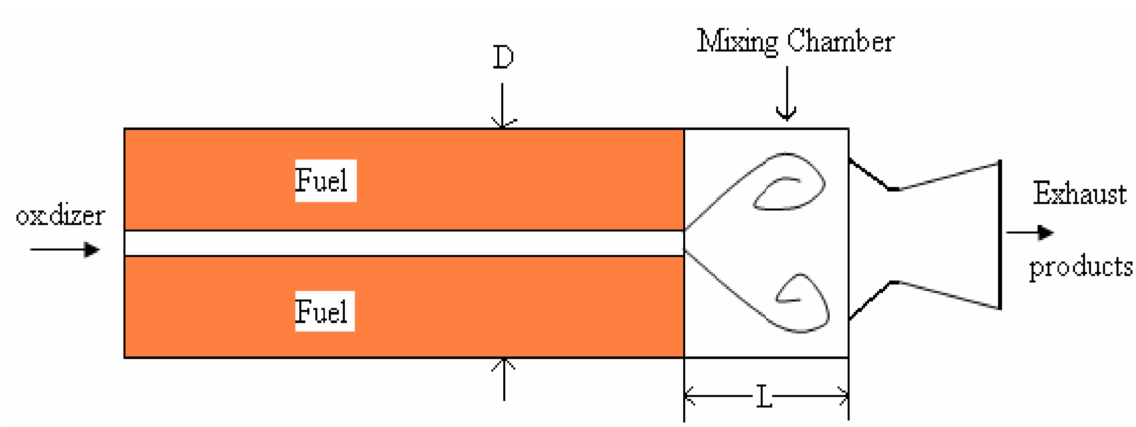

Figure 5 Sketch of the fuel grain and the mixing chamber.

2.4 Test procedure

Every experimental test followed the same procedure for testing. First, the oxygen tank was rolled out and secured to the blast wall. Then, the test stand was rolled out and secured by placing metal brackets behind the wheels. All the electronic equipment was then setup and checked to make sure it was functioning. The fuel grain was then weighed and secured into the combustion assembly with the restrictor plate. The test supervisor would open the lines for the oxidizer and propane tanks and pressurize the lines. The calibration officer would then calibrate the strain gauge with known weights.

Once the calibration was done, the test supervisor would set the oxidizer regulator to the desired supply pressure. Next, the oxidizer and propane timers were set to the desired amount of time for firing. All personnel were then evacuated behind the blast wall. The test supervisor then connected the spark plug. When the area was clear, the calibration officer started the video recording and collected data. Then, the test supervisor armed and fired the rocket. After the test was done, the test supervisor disconnected the spark plug and all recording equipment was stopped. The fuel grain was allowed to cool, taken off of the assembly, and weighed. Finally, the propane and oxidizer lines were depressurized. The checklist for conducting tests can be found in the Appendix.

2.5 Test summary

Research began in September 2005 and continued until February 2007. Several setbacks occurred during that time period that prevented data collection. Problems included instrumentation, mechanical failures, and combustion instability. After all testing had been done; twenty six lard tests were completed with supply pressures of 320 to 460 psig.

Instrumentation problems caused delays in data collection. A new A/D converter card for the system contributed to most of the instrumentation problems. After the new A/D card was installed, a problem occurred in which the entire system would freeze up and have to be rebooted when the rocket was fired. Each electrical component of the system was individually examined and observed. The problem was found to be in the spark plug. When the spark plug was activated, it created an electrical arc to the premixing chamber wall because it was so close to it. The electrical surge then traveled up the pipes, to the pressure transducers, and into the A/D card. The surge would freeze up the card and the computer, and no data could be collected. This problem was solved by changing the short spark plug with a longer one. Another problem that occurred with the new A/D card was that the strain gauge output was extremely noisy. The noise was thought to be from a 60 Hz frequency picked up from the power source but was mainly a sensitivity issue. The issue was resolved by calibrating around seventy five percent of the strain gauge maximum output to the maximum thrust output in the test.

The lard was tested with nitrous oxide as the oxidizer. None of the tests were truly successful. In all the tests, the combustion never stabilized. The problem was that the nitrogen suppressed the combustion. The combustion pressure needed to be much higher for combustion to occur. Using the equation for the characteristic velocity, equation 4:

$$c^* = \frac{P_c A_t}{\dot{m} g_o} \tag{4}$$

the combustion pressure, P_c, can be increase by decreasing the throat area, A_t. Three new graphite nozzles were made with each one having a smaller throat area than the one being used. The combustion pressure greatly increased, but not high enough for stable combustion under our test assembly. The combustion pressure needed for combustion could be reached with our nozzles and setup, but the pressures would be reaching the limits of the test stand. Thirteen N_2O tests were done in all with lard as the fuel.

Chapter III

Experimental Results and Analysis

3.1 Combustion Analysis

Combustion was a key factor to successful testing. Inadequate combustion led to unreliable test data. The combustion efficiency of the propellants was largely dependant on the equivalence ratio, defined as:

$$\Phi = \frac{O/F}{(O/F)_{stoi}} \tag{5}$$

where O/F is the oxidizer to fuel ratio at actual and stoichiometric conditions. For equivalence ratios greater than unity, the combustion was fuel-lean, and if less than unity, the mixture was fuel-rich.

In the hybrid combustion chamber, oxygen flows down the port and reacts in the boundary layer near the surface of the solid fuel. Figure 6 shows a schematic of the boundary layer combustion zone in a hybrid rocket. Combustion was achieved by oxygen being transported into the flame zone from the free stream by diffusion and flow turbulence and the fuel moving into the flame zone as a result of vaporization at the surface.

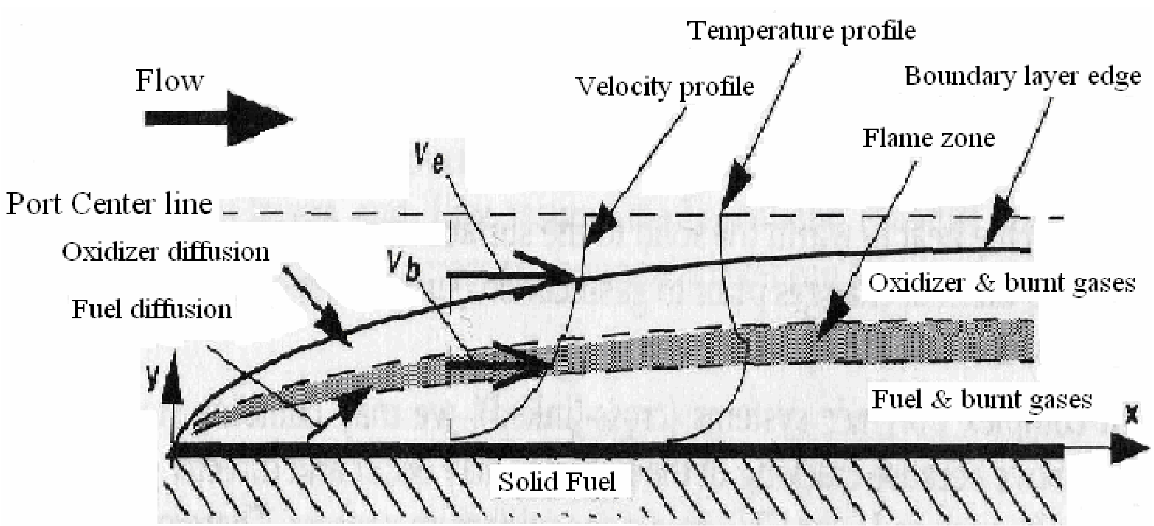

Figure 6 Combustion boundary layer for hybrid rocket.

The flame zone was formed where the equivalence ratio reached a level at which combustion would occur. The flame thickness was determined predominantly by the oxidation reaction rate.

3.2 Regression Rate Analysis

The regression rate of hybrid rockets is a parameter that shows the rate at which the fuel is consumed. For our experimental analysis, the average regression rate was calculated for each test because the regression rate varies, to an extent, down the combustion port. The average regression rate was found as the difference in the final grain thickness and the initial grain thickness divided by the burn time, as shown in equation 6.

$$\dot{r} = \frac{\delta_{gi} - \delta_{g\,f}}{t_b} \tag{6}$$

The initial grain thickness and burn time were known parameters. The average final grain thickness was estimated by using the fuel density, final fuel mass, and the known dimensions of the grain. (shown in Appendix A)

The regression rate is normally shown as a function of other parameters, such as oxidizer mass flux rate, propellant flux rate, oxidizer mass flow rate, and combustion pressure. The most common regression rate expression used in rocket propellants gives the rate as a function of the oxidizer mass flux rate, as shown in equation 7.

$$\dot{r} = aG_{ox}^{n} \tag{7}$$

The constants a and n are experimentally obtained. Combustion pressure has been shown to have little effect on the regression rate in some studies, but has had an effect in other studies. For hybrids, not enough research has been done to describe the effect of combustion pressure on the regression rate with certainity.[1,2]

Nevertheless, a regression rate equation is important in designing an engine for a given application. A propellant with a high regression rate will make a rocket have less weight because less propellant surface area will be required. Regression rate expressions can be used to compare the performance of different fuels.

3.3 Mass Flow Rate Analysis

The oxidizer mass flow rate was a key parameter determined during this testing. The specific impulse, equivalence ratio, thrust, and regression rate all depend on the mass flow rate. The average oxidizer mass flow rate was calculated using the pressure differential across an orifice plate. The average upstream supply pressure and the ambient temperature were input into a Matlab code to produce a table of the oxidizer mass flow rate for different pressure differentials. The equation used to calculate the oxidizer mass flow rate is shown in equation 8. The exact process in calculating the oxidizer mass flow is found in Appendix B.

$$\dot{m}_{ox} = \frac{e * C * A_o * \sqrt{(2 * \rho * \Delta P)}}{\sqrt{(1-\beta^4)}} \qquad (8)$$

Figure 7 show the pressure differential for test 158. The pressure difference was scattered because two separate pressure transducers were used with each having different fluctuations. Also, the pressure transducers have an inaccuracy of ±0.4% of the full scale output of 1000 psig, which means that the pressure transducers could be off by ±4 psig. That had a significant effect on the calculated oxidizer mass flow rate. Table 1 shows the uncertainty in a typical calculation of oxidizer mass flow rate.

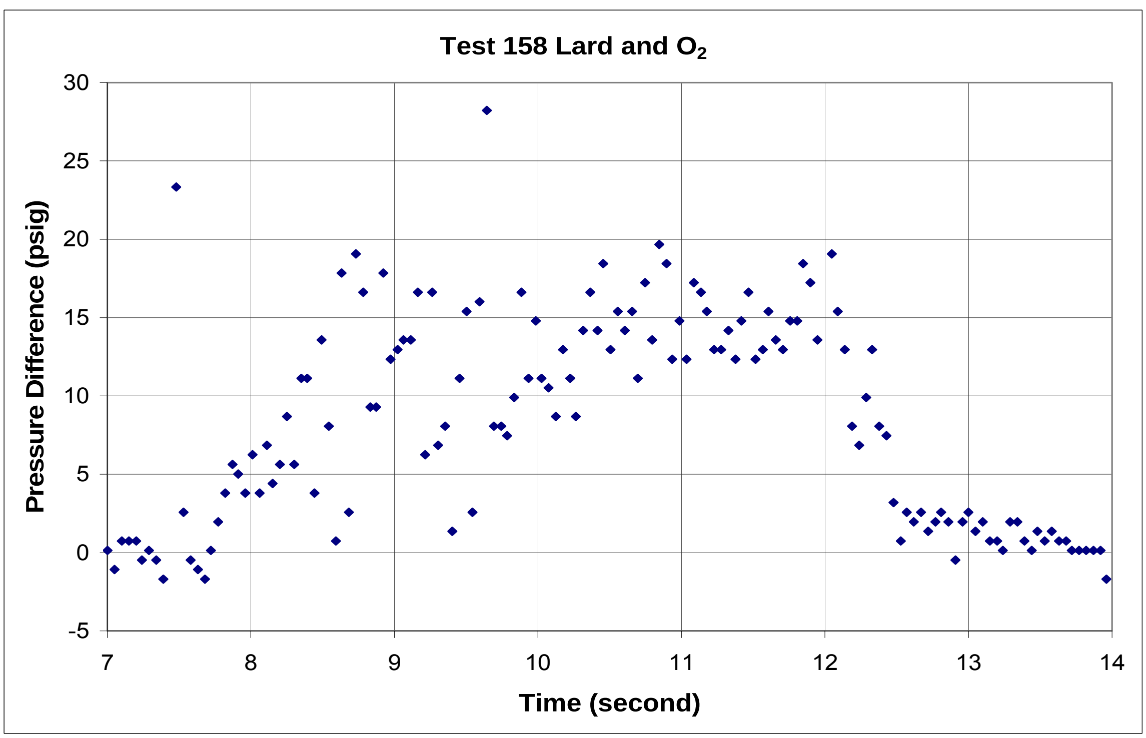

Figure 7 Pressure difference for Test 158

Table 1. Possible extremes for the oxidizer flow rate for Test 158.

	Upstream Pressure (psig)	Downstream Pressure (psig)	Pressure Difference (psig)	Oxidizer Mass Flow Rate (kg/s)	Percent Difference from Nominal
Low	174	169	5	0.0160	37%
Measured Value	178	165	13	0.0255	0%
High	182	161	21	0.0327	28%

Table 1 shows the experimental output from Test 158 with the lowest and highest possible values on the transducer accuracy. The uncertainty of the actual oxidizer mass flow rate is of concern. Table 1 shows that the oxidizer mass flow rate could be off by a tremendous amount.

3.4 Performance Analysis

In each test the thrust, supply pressure, and combustion pressure were measured to evaluate the performance characteristics of the fuel. The main performance parameter to be determined was the specific impulse.

The total impulse represents the total energy released by the propellants in a propulsion system. Integrating the thrust over the burn time the total impulse was calculated. A Riemann's Sum approximation was used to calculate the area under the thrust versus time curve for each test. Then the total impulse was used to calculate the important performance parameter, the specific impulse. The specific impulse represented the efficiency of a propulsion system. The higher it was, the better the performance. The effective specific impulse was determined by equation 9.

$$I_{sp} = \frac{\int F dt}{g_o \int \dot{m} dt} \tag{9}$$

The constant g_o was the standard acceleration of gravity at sea level, 9.8066 m/s^2 or 32.174 ft/s^2 and $\dot{m}$ represented the total mass flow rate. The force, F, represents the momentum thrust of the rocket and not the total thrust. The specific impulse was an important characteristic when comparing the performance of hybrid rocket motors to other propulsion systems.

A theoretical analysis was conducted for the combustion of lard with oxygen using two different assumptions. The first method used a frozen flow analysis, which assumed the chemical composition of the combustion products was invariant throughout the nozzle. The other method used a shifting equilibrium method that assumed the reaction went to completion in each section of the nozzle. Both methods assumed that the flow was ideally expanded with a combustion pressure of 150 psig. This analysis was carried out using a United States Air Force code.[8] Figure 8, 9, and 10 show the specific impulse, combustion temperature, and average molecular weight of the combustion products as a function of the equivalence ratio.

The frozen flow analysis underestimates the actual combustion process because it assumes zero rates of chemical reactions occur. On the other hand, the shifting equilibrium analysis overestimates the performance of a rocket by assuming the reaction goes to complete combustion. Theoretically, the actual combustion properties should be in between the two different curves of frozen flow and shifting equilibrium.

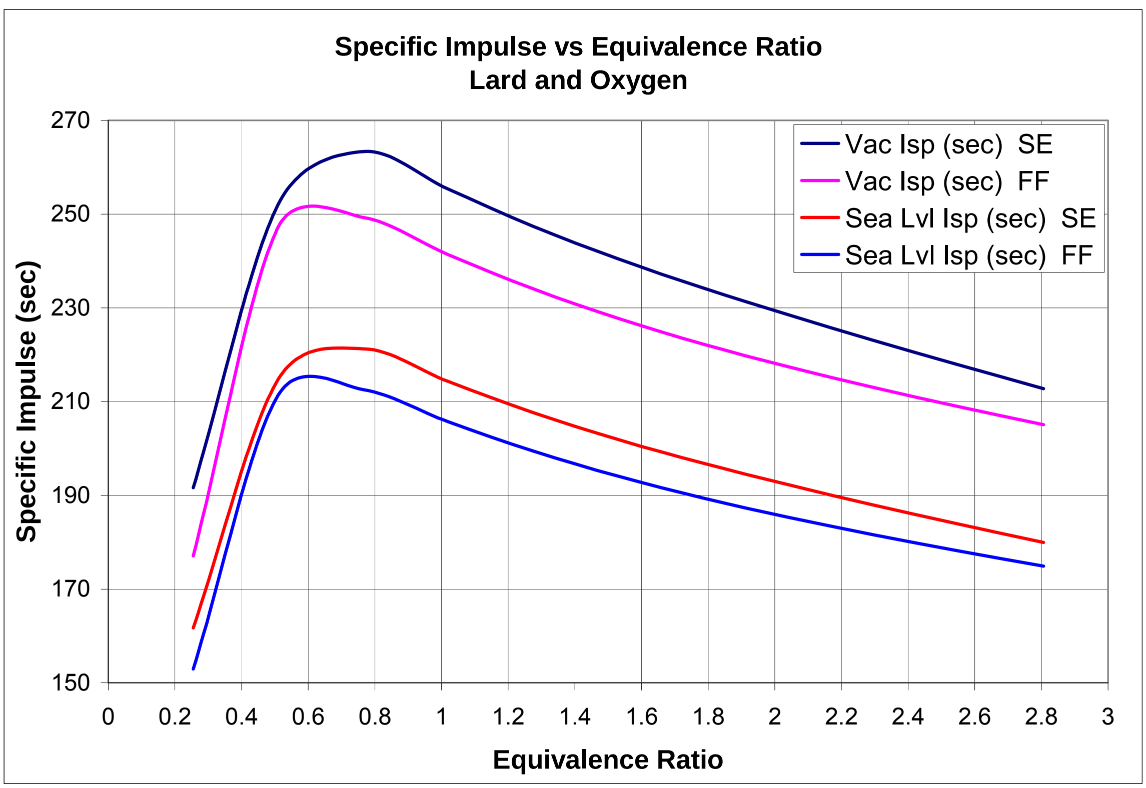

Figure 8 Theoretical specific impulse as a function of the equivalence ratio.

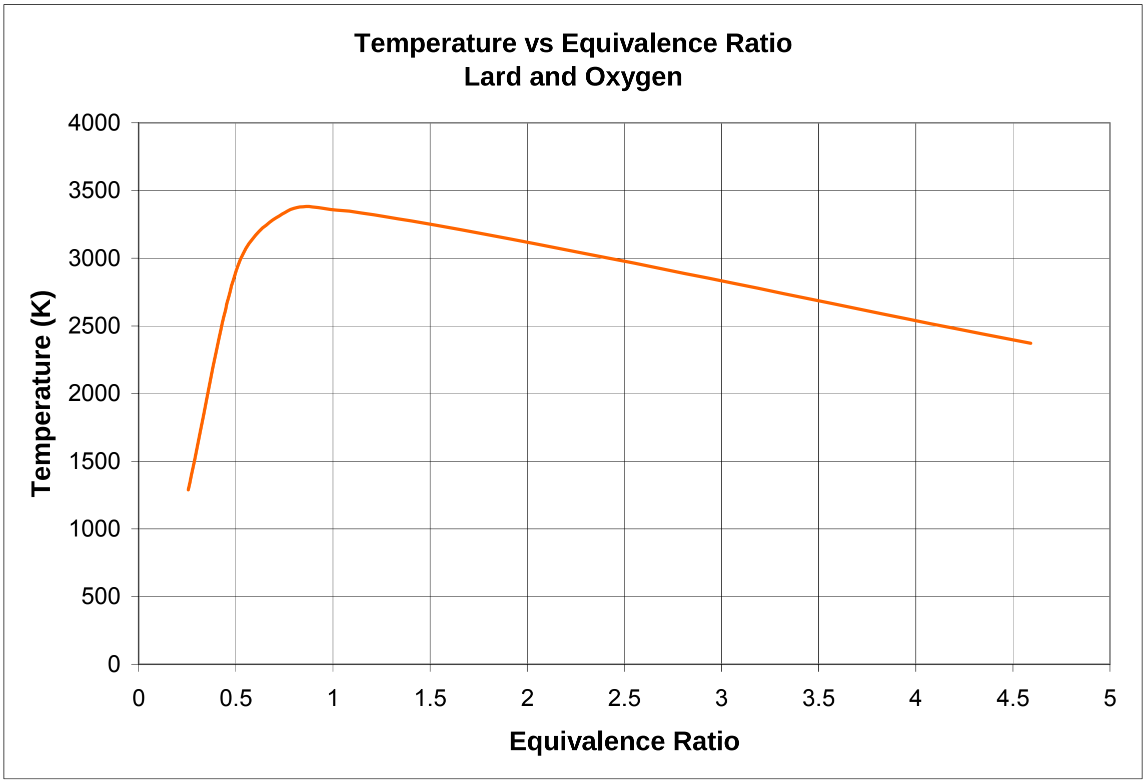

Figure 9 Theoretical combustion temperatures as a function of the equivalence ratio.

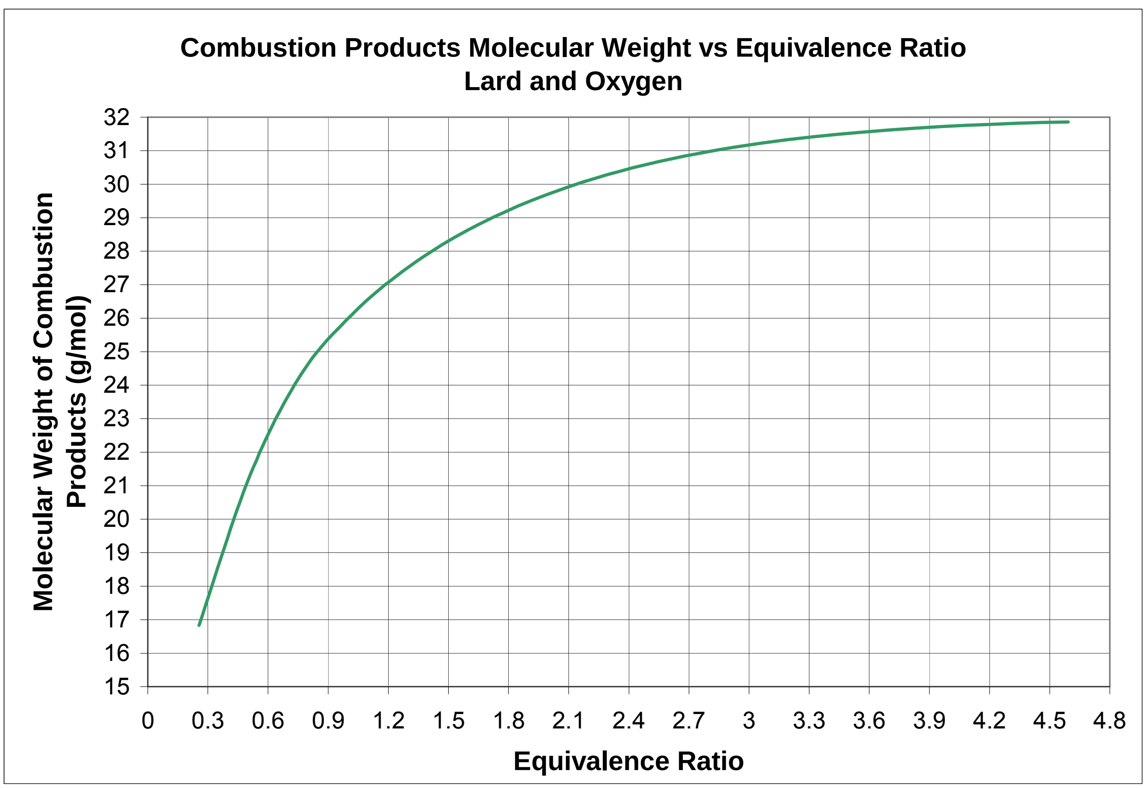

Figure 10 Theoretical molecular weight of combustion products as a function of the equivalence ratio.

The combustion temperature and molecular weight of the combustion products have a significant effect on the rocket's performance. Theoretically, the specific impulse reaches its maximum at an equivalence ratio of around 0.65, whereas, the combustion temperature obtains its maximum at an equivalence ratio of around 0.87, as shown in Figures 7 and 8, respectively. Usually, the maximum performance is reached at an equivalence ratio of unity, but here this is not the case. The reason the specific impulse is not the highest at unity can be better understood by the exhaust velocity equation 10.

$$u_e = \sqrt{\frac{2k}{k-1}\frac{R_u T_c}{\mu}\left[1-\left(\frac{P_e}{Pc}\right)^{(k-1)/k}\right]} \tag{10}$$

The exhaust velocity determines the specific impulse. Equation 10 shows that the exhaust velocity is proportional to the square root of the combustion temperature and inversely proportional to the square root of the average molecular weight of combustion products. Since the molecular weight increases with equivalence ratio, the specific impulse does not peak when the equivalence ratio is one.

3.5 Experimental Results

3.5.1 Repeatability

Repeatability tests were done to see how well test results could be reproduced under predetermined conditions. Six tests were done for a low supply pressure of 320 psig and a high supply pressure of 460 psig. All the tests were done for set oxygen supply time of five seconds with a propane supply time of half a second. Figures 11 and 12 show the plots of thrust for the low and high supply pressures. Both the low and high pressure tests tended to have a neutral, constant thrust, burn. Comparing the thrust curves, the higher pressure appeared to be more stable than the low pressure tests. This was because there was more oxidizer which produced a higher equivalence ratio. Thus, the higher equivalence ratio led to more stable combustion and less fluctuation in the thrust levels. Also, some of the instability in the thrust curve can be attributed to vibrations on the strain gauge during combustion. There was a noticeable variation in the thrust from one test to the next. Some of this difference was due to the supply tank regulator, which could have been off by plus or minus five psig.

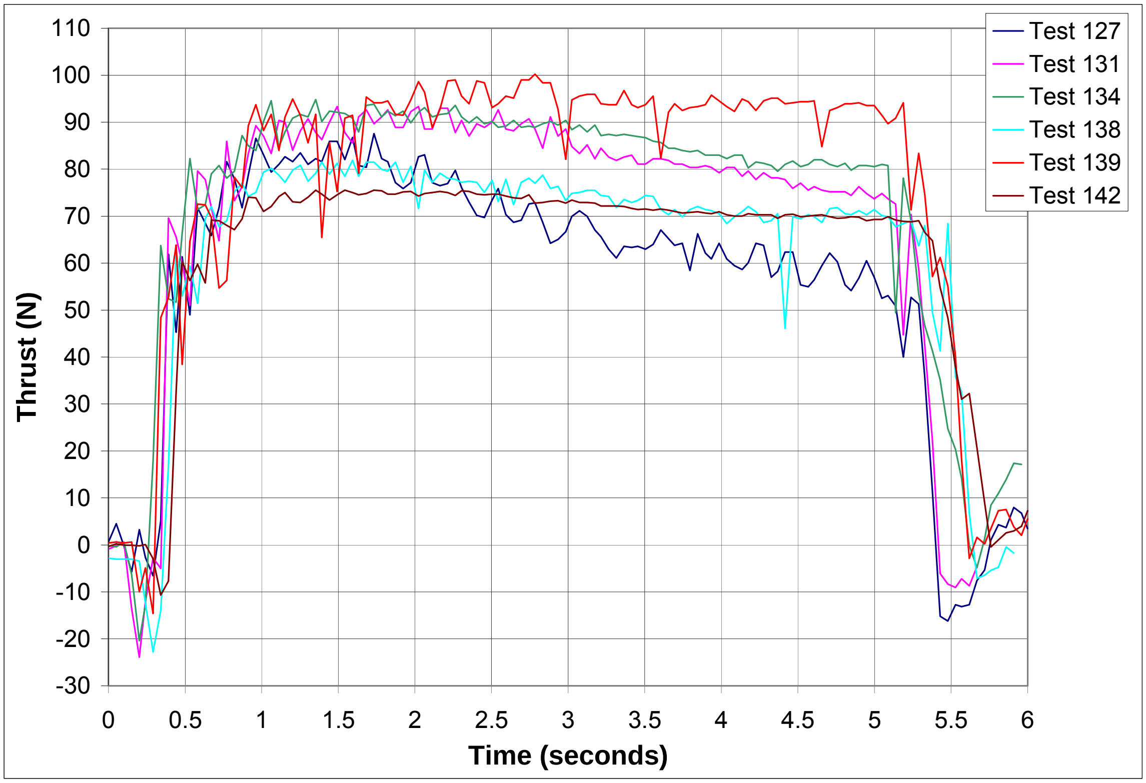

Figure 11 Measured Thrust Repeatability for an Oxygen Supply Pressure of 320 psig. (Low)

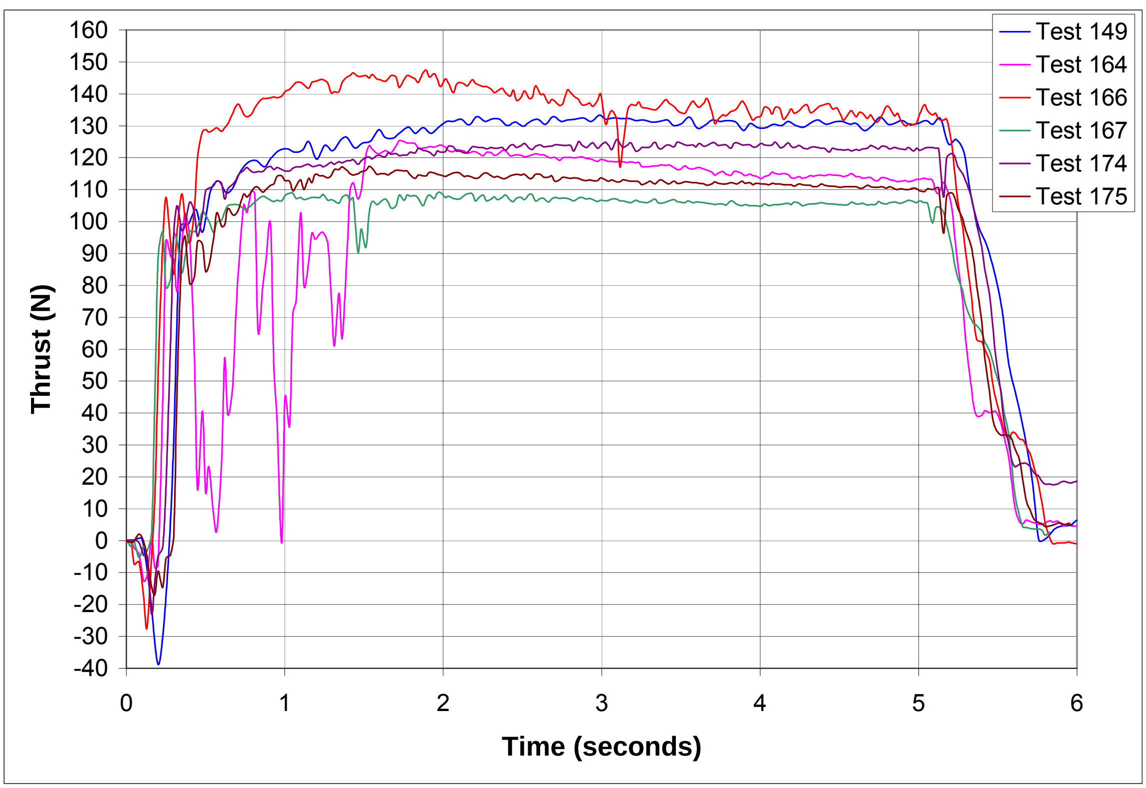

Figure 12 Measured Thrust Repeatability for an Oxygen Supply Pressure of 460 psig. (High)

Figure 13 and 14 show the plots of the combustion pressure over time for the low and high pressure tests. Both sets of tests had a considerable amount of instability. There are two main types of instabilities for hybrid motors in static tests. One is a non-acoustic oxidizer feed system-induced instability and the other is an acoustic flame holding instability.[2] The flame holding instability was stabilized by injecting propane into the pre-combustion chamber to stabilize the boundary layer flame zone. This left the oxidizer feed system-induced instability as the main contributor to the instability of the combustion pressure. The experimental setup used had several connectors in between the piping and valves creating different pressure drops down the line. A chugging type flow from the oxidizer feed system was believed to cause some of the instability.

The repeatability tests' results are better shown in Tables 2 and 3. In the tables, the average thrust and combustion pressure are shown for each test. Also, the mean and standard deviation are calculated for both the low and high pressure tests. The number of standard deviations from the mean is calculated for each test. Most of the tests were within one standard deviation from the mean. The high pressure tests did show slightly better results than the low pressure tests by having a slightly lower percent standard deviation from the mean for all both thrust and combustion pressure. The repeatability test study does show a variation in the measured data which was mainly because the supply pressure regulator cannot be set precisely to our test condition each time.

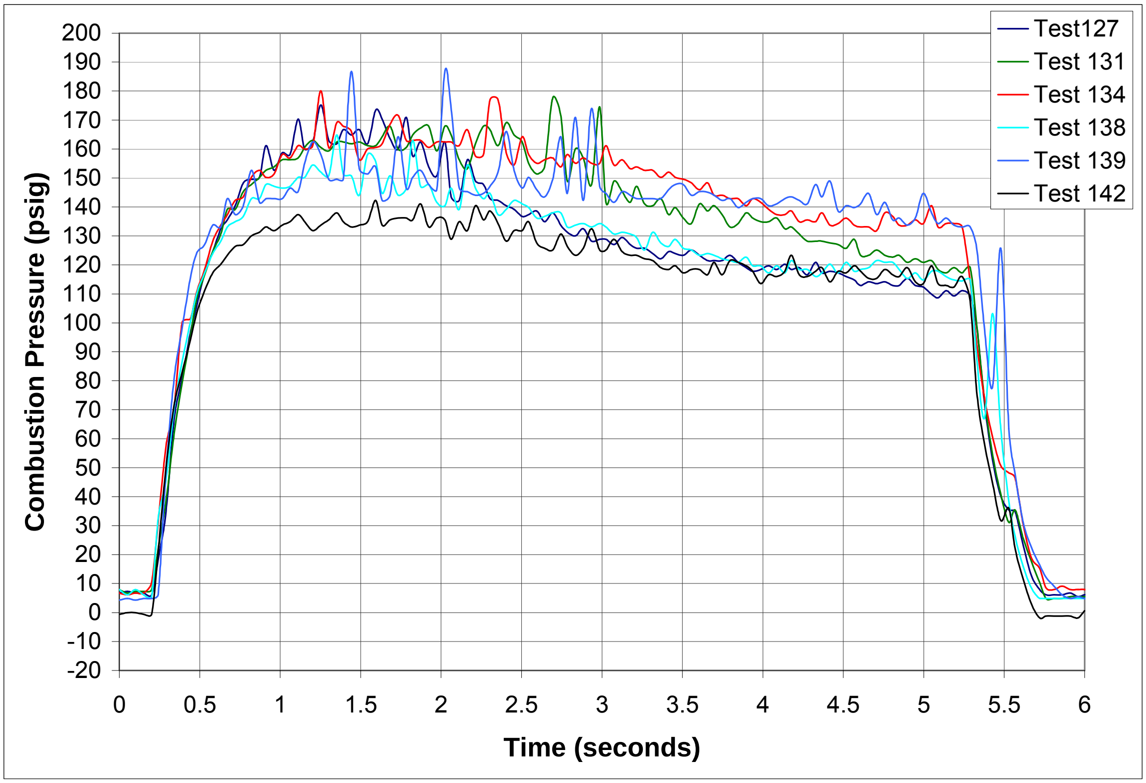

Figure 13 Combustion Pressure Repeatability for an Oxygen Supply Pressure of 320 psig. (Low)

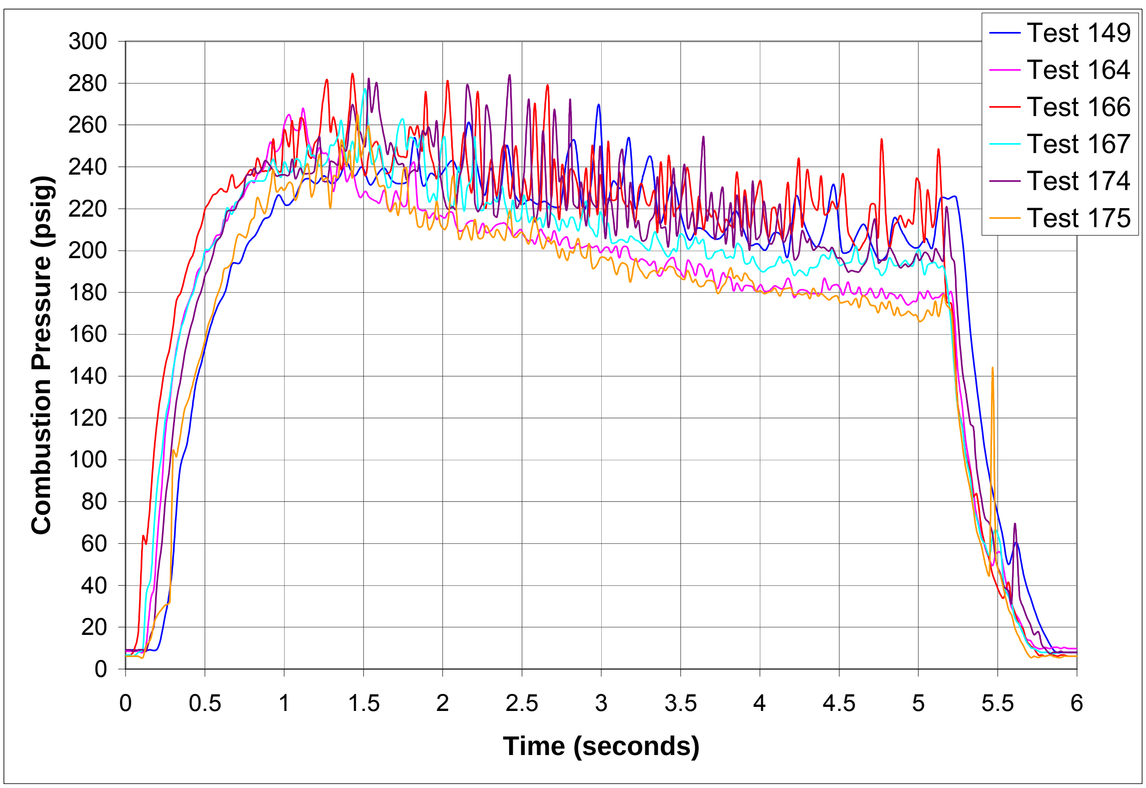

Figure 14 Combustion Pressure Repeatability for an Oxygen Supply Pressure of 460 psig. (High)

Table 2. Repeatability tests at a supply pressure of 320 psig.

	Thrust (N)	Standard Deviation from the mean	Combustion Pressure (psig)	Standard Deviation from the mean
Test 127	69.8	-1.0	125	-1.0
Test 131	84.0	0.6	147	1.2
Test 134	86.5	0.9	144	0.9
Test 138	74.5	-0.5	128	-0.7
Test 139	91.7	1.5	143	0.8
Test 142	72.3	-0.7	126	-0.9
Mean:	78.7		135	
Standard Deviation:	8.8		10	

Table 3. Repeatability tests at a supply pressure of 460 psig.

	Thrust (N)	Standard Deviation from the mean	Combustion Pressure (psig)	Standard Deviation from the mean
Test 149	117.6	-0.3	188	-1.3
Test 164	128.6	0.7	214	0.4
Test 166	137.4	1.5	222	0.9
Test 167	106.1	-1.3	204	-0.3
Test 174	121.9	0.1	214	0.4
Test 175	112.5	-0.7	186	-1.5
Mean:	120.7		208	
Standard Deviation:	11.3		15	

3.5.2 Specific Impulse

The experimental results for the specific impulse as a function of the equivalence ratio were compared to the theoretical results, seen in Figure 15. The experimental results are found to be significantly lower then the theoretical results. A few points are within the theoretical range, and several are within ten percent of the theoretical. However, most the points are not within a 10% margin of error. Uncertainty bars were put on some of the lower experimental points. The average uncertainty of the specific impulse was found to be 16.8 seconds are about 10%. The uncertainty bar covers the range of possible oxidizer mass flow rate values that would change the equivalence ratio. These lower points still do not fall in the theoretical range with the uncertainty bar. However, the oxidizer mass flow rate affects the calculated specific impulse also, which means as is depicted by the vertical uncertainty bars.

A number of factors could have contributed to the lower experimental specific impulse. The main contributor to uncertainty was the uncertainty in the oxygen mass flow rate. Also, combustion instability was a contributing factor. Cracks and bubbles in the fuel grain are not catastrophic like in solid rockets but may degrade to the rocket's performance. Also, any fuel which flashes off and exits the engine unburned will degrade the experimental specific impulse.

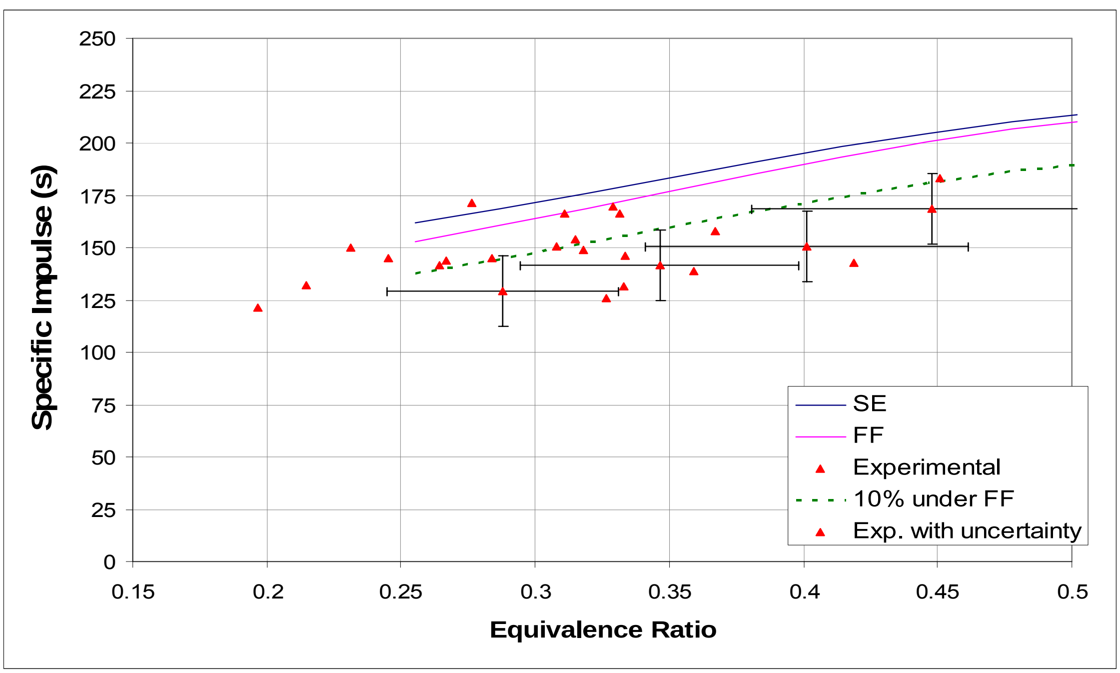

Figure 15 Comparison of experimental and theoretical specific impulse.

3.5.3 Thrust

The thrust of a rocket is the force produced by ejecting small masses at high velocities out of the rocket. Two components make up the thrust of a rocket, the momentum thrust and the pressure thrust, show in equation 11.

$$F = \dot{m}V_e + (P_e - P_a)A_e \tag{11}$$

The terms Ve, Pe, and Ae represent the exit velocity, pressure and area of the nozzle, where Pa defines the ambient pressure. The momentum thrust is the product of the total mass propellant flow rate and the exit velocity. The second component, the pressure thrust, is the difference between the exit exhaust pressure and the ambient fluid pressure times the exit area of the nozzle. The momentum thrust is typically the larger of the two components. The pressure thrust can be positive or negative. A negative pressure thrust is produced when the ambient pressure is larger than the exit pressure. Usually, the rocket nozzle is designed to have an exit pressure equal to or slightly higher than the ambient pressure.

The thrust was an important parameter because it determines how much payload a rocket can carry. The measured thrust for the experiments conducted ranged from 70 to 145 Newtons. The nozzle used for the tests was well designed, producing an average calculated pressure thrust for the tests of zero Newtons, which makes it negligible, leaving only the momentum thrust. Figure 16 was a plot of the total thrust as a function of the combustion pressure. The experimental data followed an exceptionally linear pattern. The momentum thrust increases linearly with the combustion pressure, as would be expected. Referring back to characteristic equation (4), the velocity was found to be proportional to the combustion pressure. Figure 17 was a plot of the momentum thrust vs the propellant mass flow rate. The data followed generally followed a linear trend but was scattered a small amount. Errors in the thrust measurement and oxidizer mass flow rate contributed to the scatter of the experimental data.

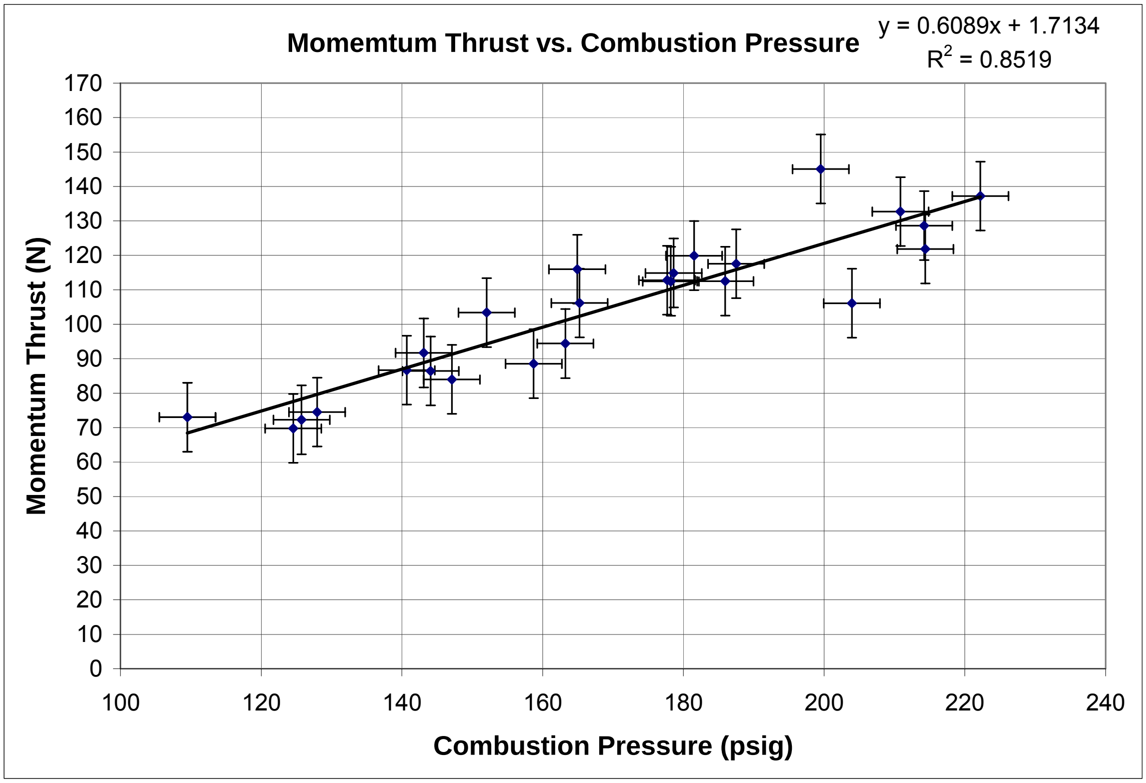

Figure 16 The momentum thrust as a function of the combustion pressure.

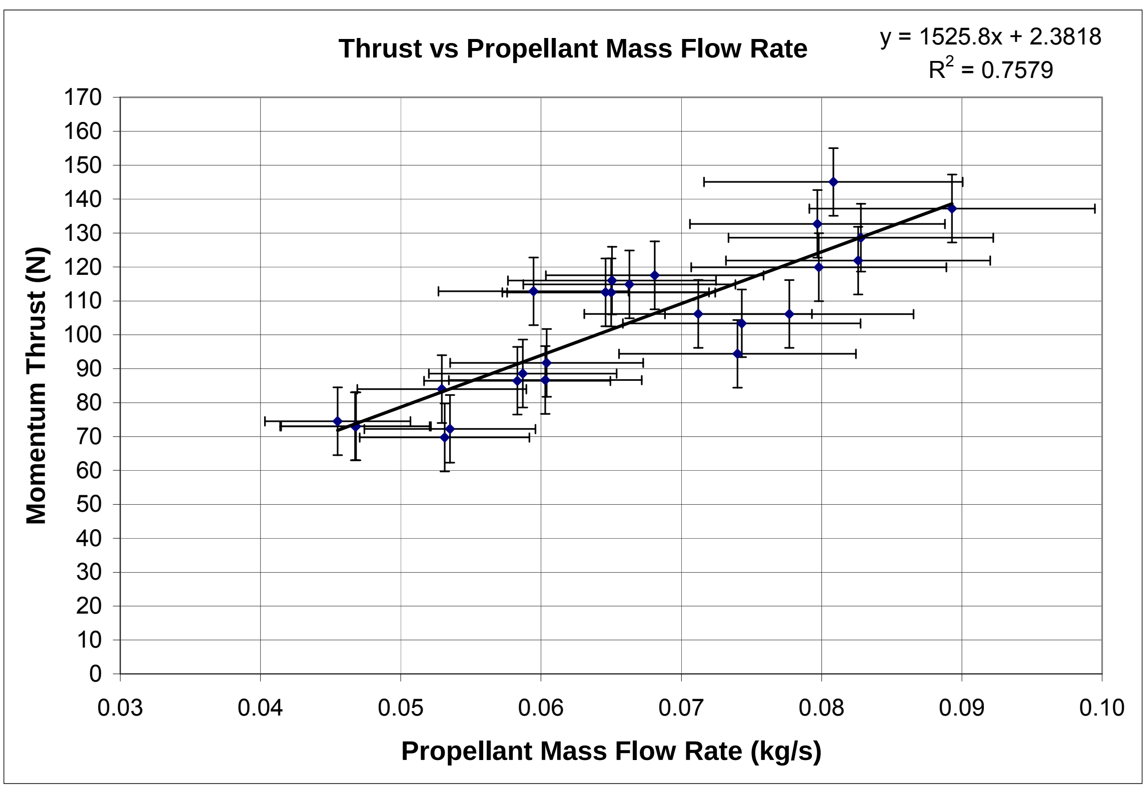

Figure 17 The momentum thrust as a function of the propellant mass flow rate.

3.5.3 Oxygen Mass Flux

The regression rate as a function of the mass flux of oxygen is very scattered but generally shows a decreasing trend, as shown in Figure 18. The low equivalence ratio that the rocket operated at was the main reason for this. There was not enough oxidizer in the aft mixing chamber to burn the excess fuel. Thus, the excess fuel was pushed out through the nozzle and did not contribute to the thrust or the combustion pressure. The reason why the oxygen mass flux was scattered can be better understand by equation (12).

$$G_{ox,av} = \frac{\dot{m}_{ox,av}}{A_{p,av}} \tag{12}$$

The oxygen mass flux increases as the oxidizer mass flow rate increases. The average port area was found calculated from the consumed fuel mass, which was higher than the amount actually burned (due to spallation or other mechanical removal of the fuel). The area of the port should be smaller than what was calculated. The degree to which it should have been smaller, depends on the amount of excess fuel not contributing to the combustion. Also, the real regression rate should be slightly lower than what has been calculated because of the unburned fuel. Therefore, the regression rate would decrease while the mass flux oxidizer would increase and produce an increasing pattern. Also, the actual oxidizer mass flow rate was higher than the value calculated which would increase the mass flux oxidizer.

In terms of regression rates, lard appears to have a significant advantage when compared to other hybrid rocket fuels using oxygen as the oxidizer. Its regression rates are around five times higher than those similar mass flux oxidizers. The high regression rates were partially due to the high heat of combustion of lard. Lard has a heat of combustion of 39.6 MJ/kg comparable to that of jet fuel (42.8 MJ/kg).

The regression rate as a function of the mass flux oxidizer may not a good relationship to use because the geometry cannot be physically interpreted. It relies on the geometry, which changes with the flow. Plus, our experiments only examined one grain length, whereas other studies examined multiple grain lengths. Since the mass flux oxidizer was not a good relationship to use in our case, some other relationships were examined.

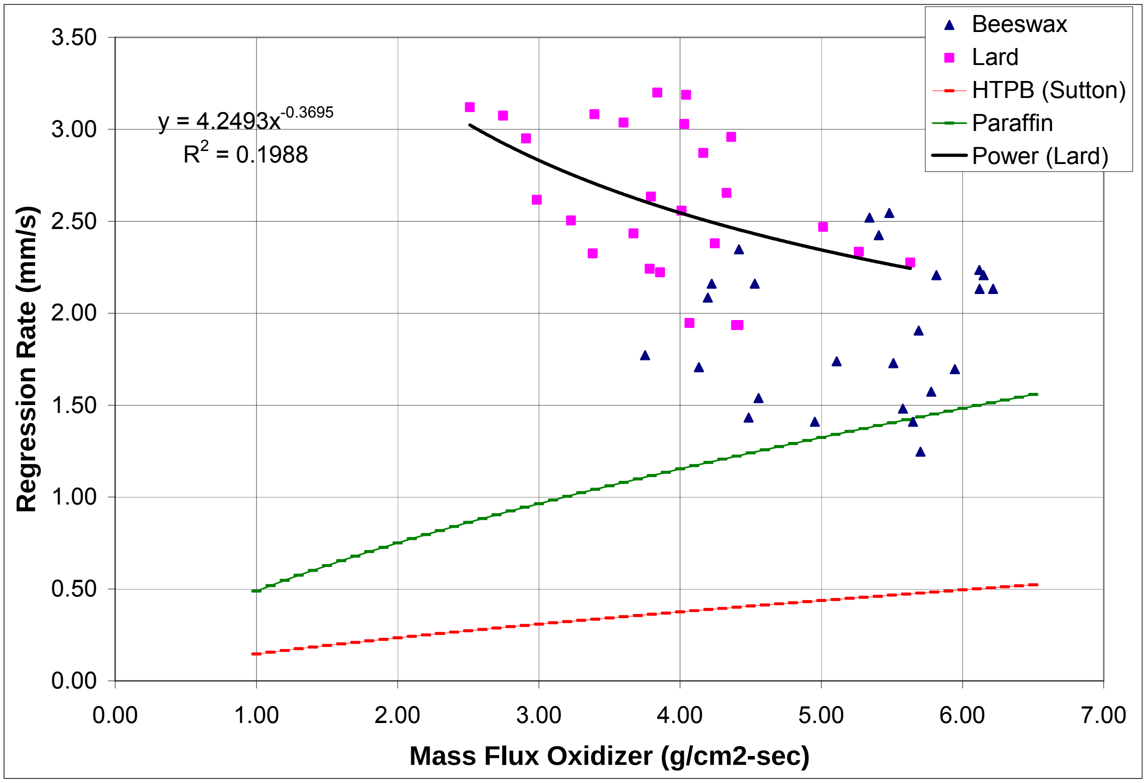

Figure 18 Comparison of regression rates as a function of the mass flux oxidizer.

<u>3.5.4 Experimental Correlation of Regression Rates</u>

As discussed previously, hybrid rocket fuel regression rates are commonly found to correlate with the oxidizer mass flux rate. However, in the present study, the results are scattered, as can be seen in Figure 18. This may be related to fuel spallation and the ejection of unburned fuel from the engine. Since the oxygen mass flux rate was not found to be a reliable means of predicting regression rate, some other relationships were examined, and the regression rate was found to correlate nicely with the oxidizer mass flow rate and the total propellant mass flow rate (Fig. 19 and 20). The trend lines were found to fit the form:

$$\dot{r} = 43.552\dot{m}_{ox}^{\ 0.7671} \tag{12}$$

$$\dot{r} = 20.333\dot{m}_{prop}^{\ 0.7552} \tag{13}$$

These equations can be used to predict the regression rate for our test apparatus, using lard and oxygen as the propellants, just by knowing the oxidizer mass flow rate or the total flow rate. The R^2 statistic used to measure how well the data fit the model of the power curve was calculated to be 0.7653 for the oxidizer mass flow rate and 0.967 for the total propellant mass flow rate, which shows a good relationship with the experimental data.

An uncertainty analysis was done on the regression rate and mass flow rates (shown in Appendix C). The uncertainty of the regression rate was found to have an average of 0.318 mm/s or 10.7%. Whereas the average uncertainty in the oxidizer mass flow rate and total mass flow rate were 32.5% and 11.4%, respectively. The uncertainty ranges are shown graphically in Figures 19 and 20. Also, the average deviations between the correlation equations and the actual data were calculated. The average deviation of the data from the first correlation equation was 7.8% for the oxidizer mass flow rate and 6.6% for the regression rate. For the second correlation, using the total mass flow rate, the average deviation of the data from the equation was 3.6% for the total mass flow rate and 2.6% for the regression rate. Table 4 shows the comparison of the average uncertainties and deviation from the correlations. The average deviation was within or close to the average uncertainty of the calculated data.

At first appearance, lard appears to have a significant advantage over many other hybrid fuels, since over a wide range of oxidizer mass flux rates, it provides a regression rate several times higher than the other fuels (Fig. 18). However, these high regression rates are likely due, at least in part, to the loss of unburned fuel from the engine. This view is supported by the fact that the experimentally determined specific impulses are significantly below their predicted values.

Table 4. The average uncertainty of the calculated experimental data and the average deviation from the experimental data to the correlation.

	Average Uncertainty	Average Deviation from Correlation Eq. (12)	Average Deviation from Correlation Eq. (13)
Regression Rate (mm/s)	10.7%	6.6%	2.6%
Oxidizer mass flow rate (kg/s)	32.5%	7.8%	______
Total mass flow rate (kg/s)	11.4%	______	3.6%

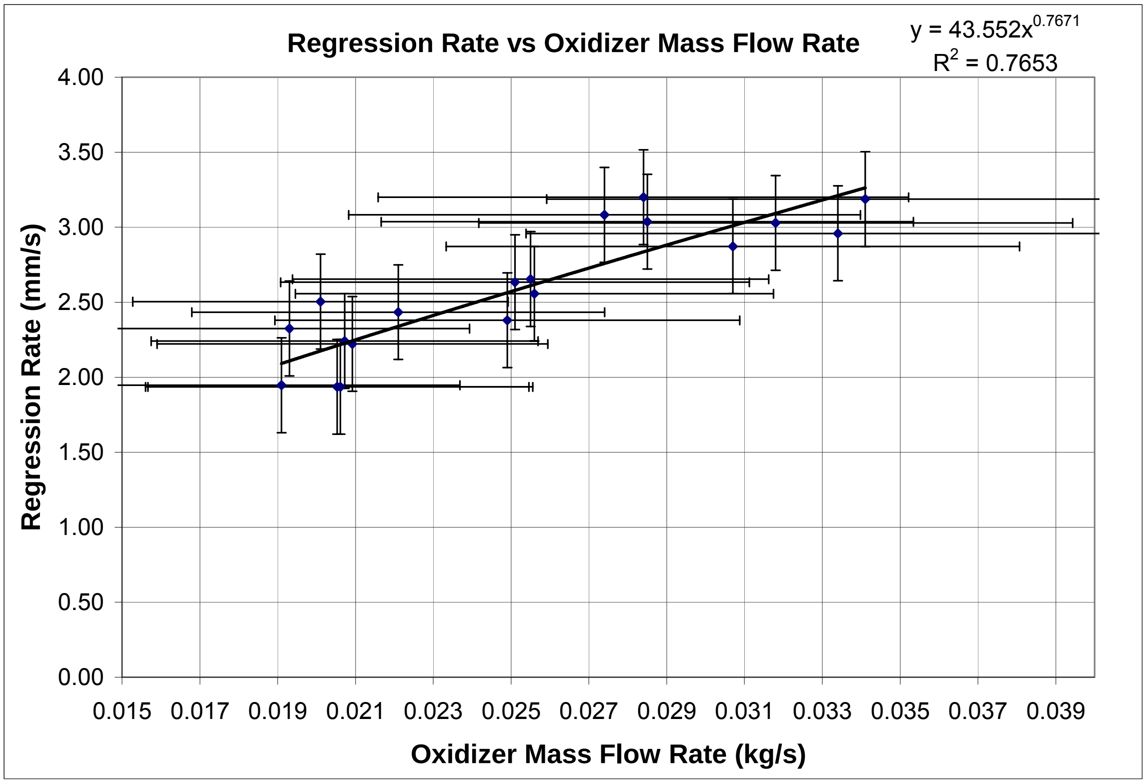

Figure 19 The regression as a function of the oxidizer mass flow rate with uncertainty bars.

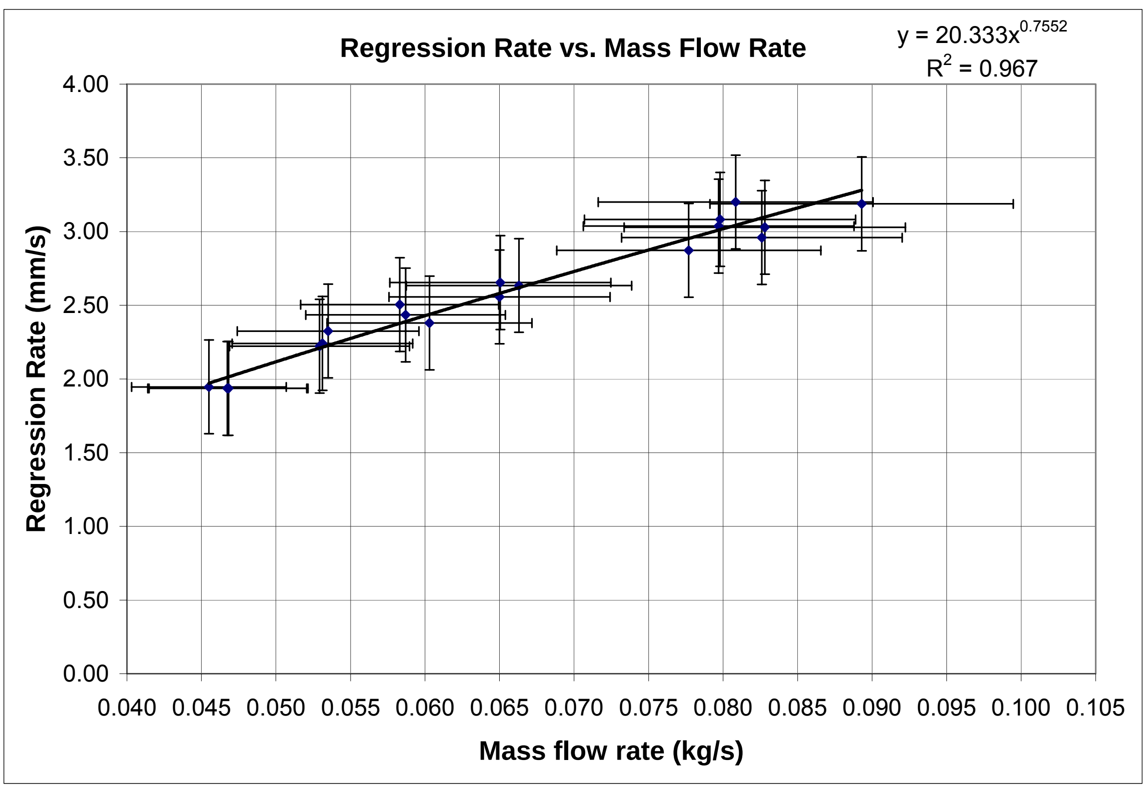

Figure 20 The regression rate as a function of the total mass flow rate with uncertainty bars.

Chapter IV
Summary & Conclusions

Lard has been tested successfully in a lab scale hybrid rocket facility at the University of Tennessee-Knoxville. Tests were conducted at combustion pressures ranging from 110 to 222 psig and equivalence ratios from 0.2 to 0.45. Experimentally determined specific impulses ranged from 121 to 183 seconds. These values were significantly lower than would be expected based on analytical modeling. The disparity between theoretical and experimental results seemed to become more pronounced at higher equivalence ratios. The cause for the difference remains uncertain but it is believed to result, at least in part, from spallation of the fuel and the ejection of unburned fuel particles from the engine.

More experimental testing needs to be conducted to evaluate the practicality of lard as a fuel for hybrid rocket motors. It is recommended that improvements in the instrumentation and test stand need to be made. In addition, more tests at higher pressures and thrust levels should be conducted. This would require adaptations to the test stand to operate at higher pressures. Specifically, the thrust measurement system would require modification, since it has already been operating near its maximum capacity. In addition, a means should be developed to dampen out oscillations and, thereby, reduce noise in the data.

Also, several tests need to be conducted using different length fuel grains to determine if a lengthened mixing chamber would allow more complete combustion and provide improved specific impulse. The oxidizer mass flow rate needs to be better estimated because of its importance. Either a pressure differential or mass flow rate meter should be installed to better estimate the oxygen flow rate. A high temperature thermocouple that can be used in an oxidizing environment needs to be installed in the combustion chamber or nozzle exit plane. This thermocouple would be a valuable addition to compare the theoretical and experimental combustion temperature.

Performance may be enhanced by increasing the equivalence ratio. The current research was operated in a very fuel rich environment. It is possible that more oxidizer is needed to obtain higher equivalence ratios. This could be done by inserting an additional oxidizer line in the precombustion chamber. However, it is also possible that this will further degrade performance by increasing fuel spallation and the loss of unburned lard. Overall the testing of lard and oxygen as a possible hybrid rocket propellant combination was encouraging. However, more study does must be done before lard can become a commonly used fuel.

References

1. Sutton, G. P., Biblarz, O., Rocket Propulsion Elements. 7th ed. New York: John Wiley and Sons, 2001.
2. Humble, R.W., Henry, G. N., Larson, W.J. Space Propulsion Analysis and Design. 1st ed. Revised. New York: The McGraw-Hill Companies, Inc., 1995.
3. Karabeyoglu, M.A., Zilliac, G., Cantwell, B.J., De Zilwa, S., Castelluci, P. "Scale-Up Tests of High Regression Rate Liquefying Hybrid Rocket Fuels". AIAA Paper 2003-1162.
4. De Zilwa, S., Zilliac, G., Karabeyoglu, M. A. and Reinath, M., "Time-Resolved Fuel-Grain Measurement in Hybrid Rockets", 39th AIAA/ASME/SAE/ASEE Joint Propulsion Conference, 20-23 July, 2003, Huntsville, AL.
5. Frolik, Steven. "Hybrid Rockets." Aerospace America, Dec. 2005.
6. Damian, P., Pontius, FW., "From rocket to remediation: The perchlorate problem". Environmental Protection, Vol. 10, no. 6, pp. 24-31, June 1999.
7. Dariento, Laurence, "Rocket fuel's spread in water could be worse than thought". Los Angeles Business Journal, 12 May 2003.
8. Selph, Curtis. Air Force Equilibrium Specific Impulse Code. United States Air Force (1992).
9. Scholes, Joshua. "Bio-derived Fuels for Hybrid Rocket Motors." Thesis at the University of Tennessee-Knoxville 2005.
10. Adebanjo, Adenike. "Production of Fuels and Chemicals from Biomassderived Oil and Lard." University of Saskatchewan 2005.
11. Aftergood, Steven. "Propellants." 14 Jan. 2007<http://www.fas.org/nuke/control/mtcr/ text/mtcrhandbookitem4.pdf >

Appendix

Appendix A: Data Calculations
The regression rate is the change in grain thickness per unit time:

$$\dot{r} = \frac{\delta_{gi} - \delta_{g\,f}}{t_b} \tag{14}$$

The initial thickness and the burn time are known, the only parameter needed to be calculated in the regression rate was the final grain thickness. It was assumed that all burning took place along the port with no burning on the ends. The final grain thickness was determined using the volume definition:

$$V = \frac{M_{final}}{\rho_f} \tag{15}$$

where the final mass and fuel density are known.
The volume can be solved by estimating it as the volume of a cylinder:

$$V = \pi * \frac{OD^2}{4} * L_g - \pi * \frac{D_f^{\ 2}}{4} * L_g \tag{16}$$

The only unknown parameter was the final port diameter. This was calculated by combining equation (15) and equation (16) into the equation:

$$D_f = \sqrt{(OD^2 - \frac{4M_{final}}{\pi \rho_f L_g}} \tag{17}$$

The final grain thickness was calculated using the difference between the outer grain diameter and the final port diameter:

$$\delta_{gf} = \frac{OD - \sqrt{OD^2 - \frac{4M_{final}}{\pi \rho_f L_g}}}{2} \tag{18}$$

Then the regression rate was calculated inserting equation (18) into the regression rate equation (14).

Total impulse was found as the integrated result of thrust as a function of time.

$$I = \int_{t=0}^{t=tb} T dt \tag{19}$$

A Riemann squares approximation was used to determine the area under the impulse curve:

$$I = \sum_{i=0}^{tb} \frac{1}{2} (T_{i+\Delta t} + T_i)(t_{i+\Delta t} - t_i) \tag{20}$$

The specific impulse was calculated by the total impulse and burned propellant mass:

$$Isp = \frac{I}{g(m_f + m_{ox})} \tag{21}$$

The exit velocity was calculated by the burned propellant mass and the measured thrust:

$$u_e = \frac{T_{ave} - T_{press}}{m_f + m_{ox}} \tag{22}$$

The mass flow rate of the fuel was calculated as the change in mass per unit time:

$$\dot{m}_f = \frac{M_{initial} - M_{final}}{t_b} \tag{23}$$

The mass flow rate of the propellant is the sum of the oxidizer and fuel flow rates:

$$\dot{m}_p = \dot{m}_{ox} + \dot{m}_f \tag{24}$$

The fuel ratio was calculated as:

$$O/F = \frac{\dot{m}_{ox}}{\dot{m}_f} \tag{25}$$

The equivalence ratio was determined by:

$$\phi = \frac{O/F}{\left(O/F\right)_{stoich}} \tag{26}$$

The stoichiometric oxidizer to fuel ratio is determined using

$$\left(O/F\right)_{stoich} = \frac{moles_{ox}}{moles_f} * \frac{\mu_{ox}}{1mole_{ox}} * \frac{1mole_f}{\mu_f} \tag{27}$$

The stoichiometric oxidizer was calculated to be 1.96.

The molecular ratio was found from the stoichiometric chemical reaction balance:

$$1 * C_x H_y + aO_2 \rightarrow xCO_2 + \frac{y}{2} H_2O \tag{28}$$

where a is the molecular ratio and is equivalent to:

$$a = x + \frac{y}{4} \tag{29}$$

The exit pressure was calculated by:

$$Pe = Pc \frac{Pe}{Pc}$$

where the pressure ratio was found to be 0.08312 for the nozzle used.

Appendix B: Oxidizer mass flow rate calculation

A Matlab code was written to calculate the oxidizer mass flow rate by inputting the upstream supply pressure. The equations below were used in the code.

The mass flow rate was calculated as:

$$\dot{m}_{ox} = \frac{e * C * A_o * \sqrt{(2 * \rho * \Delta P)}}{\sqrt{(1-\beta^4)}} \tag{30}$$

Beta ratio was the ratio of orifice plate hole diameter to pipe diameter:

$$\beta = \frac{d}{D} \tag{31}$$

The density was calculated using the ideal gas law:

$$\rho = \frac{P_{up}}{\frac{R_u}{\mu_{ox}} * T_{ox}} \tag{32}$$

The temperature of the oxidizer was assumed to be the same as the ambient temperature. The gas expansibility is determined as:

$$e = 1 - (0.41 + 0.35 * \beta^4) * \frac{\Delta P}{K * P_{up}} \tag{33}$$

The discharge coefficient for flange taps is calculated as:

$$C = \left[0.598 + 0.468 * \left(\beta^4 + 10 * \beta^{12}\right)\right] * \sqrt{\left(1-\beta^4\right)} + (0.87 + 0.81 * \beta^4) * \sqrt{\frac{\left(1-\beta^4\right)}{\mathrm{Re}_D}} \tag{34}$$

The last term in the discharge coefficient calculation was neglected in the code because it was very small compared to the other term.

<u>Matlab code used to create oxygen flow rate chart</u>

```
%Clear memory
clear all;
clc;
%%Values to be input%%
%Average upstream pressure (psig)
P=182;
%Temperature (K)
T=289;

%%Calculating variables%%
%Convert to metric units, Pa
p1=P*6894.75729317;
%Orifice plate hole diameter (m)
d=0.00568706;
%Pipe diameter (m)
D=0.0157988;
```

```
%Orifice and pipe areas   (m^2)
At=pi/4*d^2;
Ap=pi/4*D^2;
%Beta ratio
b=d/D;
%Coefficients
k=1.39;
C=(0.598 +0.468*(b^4+10*b^12))*sqrt(1-b^4);
%Gas constant for oxygen (J/kg-K)
r=260;
%Standard pressure (Pa) and temperature (K)
pst=101325;
Tst=289;
%Density (kg/m^3)
rho=p1/r/T;

i=1;
dp(i)=0;
for i=1:1:101
%Expansion coefficient
e(i)=1-(0.41+0.35*b^4)*dp(i)/k/p1;
%Flow rate (kg/sec)
qm(i)=e(i)*C*At*sqrt(2*rho*dp(i))/sqrt(1-b^4);
%Other flow rates
qa(i)=qm(i)/rho;
qs(i)=qa(i)*p1*Tst/pst/T;
%Pressure differential (Pa)
dp(i+1)=dp(i)+6894.75729317;
end
%Print chart
fprintf('\n\t\t\t\t\t\tDifferential Pressure vs. Flow Rate\n')
fprintf('\t   0\t   1\t   2\t   3\t   4\t   5\t   6\t   7\t   8\t   9\t\n')
for i=1:10:100
fprintf('%2.0f\t%5.4f\t%5.4f\t%5.4f\t%5.4f\t%5.4f\t%5.4f\t%5.4f\t%5.4f\t%5.4f\t%5.4f\n
',i-1,qm(i),...
    qm(i+1),qm(i+2),qm(i+3),qm(i+4),qm(i+5),qm(i+6),qm(i+7),qm(i+8),qm(i+9))
end
fprintf('100\t%5.4f\n',qm(101))
```

Oxidizer mass flow rate table for Test 158, which had an upstream pressure of 178 psig and oxygen temperature of 289 K.

Differential Pressure vs. Flow Rate

	0	1	2	3	4	5	6	7	8	9
0	0.0000	0.0073	0.0102	0.0125	0.0144	0.0161	0.0176	0.0190	0.0203	0.0215
10	0.0226	0.0236	0.0246	0.0256	0.0265	0.0274	0.0283	0.0291	0.0299	0.0306
20	0.0314	0.0321	0.0328	0.0335	0.0341	0.0348	0.0354	0.0360	0.0366	0.0372
30	0.0378	0.0383	0.0388	0.0394	0.0399	0.0404	0.0409	0.0414	0.0419	0.0423
40	0.0428	0.0433	0.0437	0.0441	0.0446	0.0450	0.0454	0.0458	0.0462	0.0466
50	0.0470	0.0474	0.0477	0.0481	0.0485	0.0488	0.0492	0.0495	0.0499	0.0502
60	0.0505	0.0508	0.0512	0.0515	0.0518	0.0521	0.0524	0.0527	0.0530	0.0533
70	0.0535	0.0538	0.0541	0.0544	0.0546	0.0549	0.0551	0.0554	0.0556	0.0559
80	0.0561	0.0564	0.0566	0.0568	0.0571	0.0573	0.0575	0.0577	0.0579	0.0582
90	0.0584	0.0586	0.0588	0.0590	0.0592	0.0594	0.0595	0.0597	0.0599	0.0601
100	0.0603									

Appendix C: Uncertainty Analysis

The regression rate was simplified to equation (35) for ease in analysis

$$\dot{r} = \frac{r_i}{t_b}\left[1 - \sqrt{\frac{m_f}{m_i}}\right] \tag{35}$$

r_i was the initial radius of the combustion port
t_b was the burn time
m_f was the final burned fuel mass
m_i was the initial fuel mass

The uncertainty of the regression rate was found by equation (36)

$$\omega_{\dot{r}} = \left[\left(\frac{\partial \dot{r}}{\partial r_i}\omega_{r_i}\right)^2 + \left(\frac{\partial \dot{r}}{\partial t_b}\omega_{t_b}\right)^2 + \left(\frac{\partial \dot{r}}{\partial m_i}\omega_{m_i}\right)^2 + \left(\frac{\partial \dot{r}}{\partial m_f}\omega_{m_f}\right)^2\right]^{1/2} \tag{36}$$

The uncertainty in the initial radius, initial mass, burned mass, and time of burn are shown below.

$\omega_{ri} = \pm 0.001$ m
$\omega_{mi} = \pm 0.001$ kg
$\omega_{mf} = \pm 0.05 * m_f$ kg
$\omega_{tb} = \pm 0.05$ s

The uncertainty in the instrumentation was used as the parameters for the uncertainties shown above. The final burned fuel mass uncertainty was conservatively estimated to be 5% of the total mass. The regression rate was found to have an uncertainty of 0.318 mm/s or 10.7%.

The specific impulse was simplified to equation (37) for ease in analysis

$$Isp = \frac{F \cdot t}{g_o(m_f + \dot{m}_{ox} t_b)} \tag{37}$$

g_o is the gravitational constant assumed to be 9.81 m/s2
F is the force found from the strain gauge
m_{ox} is the oxidizer mass flow rate with an average uncertainty of 32.5%

The uncertainty of the specific impulse was found by equation (38)

$$\omega_{Isp} = \left[\left(\frac{\partial Isp}{\partial F}\omega_F\right)^2 + \left(\frac{\partial Isp}{\partial m_f}\omega_{mf}\right)^2 + \left(\frac{\partial Isp}{\partial \dot{m}_{ox}}\omega_{\dot{m}_{ox}}\right)^2 + \left(\frac{\partial Isp}{\partial t_b}\omega_{tb}\right)^2\right]^{1/2} \tag{38}$$

The uncertainties in the thrust (strain gauge) and oxidizer mass flow rate are shown below.

$\omega_F = \pm 10$ N
$\omega_{mox} = \pm 0.325 * m_{ox}$ kg/s

The specific impulse was found to have an uncertainty of 16.8 seconds or 10.2%.

The deviation between the acquired experimental data and the correlation was found by equation (39).

$$\%Deviation = \frac{|Actual - Correlation|}{Correlation} x100\% \qquad (39)$$

Appendix D: Test Summary

Test	Supply Pressure (psig)	Initial Fuel Mass (kg)	Final Fuel Mass (kg)	Average Upstream Pressure (psig)	Average Combustion Pressure (psig)	Average Thrust (N)
127	320	0.585	0.423	136	125	69.8
131	320	0.585	0.425	137	147	84.0
134	320	0.585	0.394	153	144	86.5
138	320	0.585	0.453	137	128	74.5
139	320	0.585	0.381	152	143	91.7
142	320	0.585	0.414	135	126	72.3
143	360	0.585	0.408	155	141	86.9
144	360	0.585	0.402	169	159	88.6
145	360	0.585	0.340	174	165	106.2
160	360	0.585	0.454	122	110	73.0
146	400	0.585	0.323	195	182	119.9
147	400	0.585	0.388	190	178	112.5
148	400	0.585	0.379	190	179	114.9
150	440	0.585	0.443	191	178	112.9
151	440	0.585	0.349	212	200	145.1
158	440	0.585	0.407	178	165	115.6
165	440	0.585	0.360	223	211	132.7
149	460	0.585	0.330	229	214	128.6
164	460	0.585	0.398	203	188	117.6
166	460	0.585	0.309	239	222	137.4
167	460	0.585	0.350	218	204	106.1
174	460	0.585	0.339	230	214	121.9
175	460	0.585	0.413	201	186	112.5

Test	r (mm/s)	Φ	Isp (s)	Oxidizer Mass Flow Rate (kg/s)	Fuel Mass Flow Rate (kg/s)	Total Propellant Mass Flow Rate (kg/s)	Mass Flux Oxidizer (g/cm^2-sec)
127	2.24	0.33	126	0.021	0.032	0.053	3.78
131	2.22	0.33	146	0.021	0.032	0.053	3.86
134	2.50	0.27	142	0.020	0.038	0.058	3.23
138	1.95	0.37	158	0.019	0.026	0.046	4.07
139	2.62	0.25	145	0.020	0.041	0.060	2.99
142	2.32	0.29	129	0.019	0.034	0.054	3.38
143	2.38	0.36	139	0.025	0.035	0.060	4.25
144	2.43	0.31	151	0.022	0.037	0.059	3.67
145	2.95	0.23	150	0.022	0.049	0.071	2.91
160	1.94	0.40	151	0.021	0.026	0.047	4.40
146	3.08	0.27	144	0.027	0.052	0.080	3.39
147	2.56	0.33	166	0.025	0.040	0.065	4.01
148	2.63	0.31	166	0.025	0.041	0.066	3.79
150	2.27	0.45	183	0.028	0.032	0.060	5.63
151	3.20	0.28	172	0.026	0.054	0.081	3.84
158	2.65	0.33	170	0.026	0.040	0.065	4.33
165	3.04	0.28	145	0.029	0.051	0.080	3.60
149	3.03	0.32	149	0.032	0.051	0.083	4.03
164	2.47	0.42	143	0.031	0.037	0.068	5.01
166	3.19	0.32	154	0.034	0.055	0.089	4.04
167	2.87	0.33	131	0.031	0.047	0.078	4.17
174	2.96	0.35	141	0.033	0.049	0.083	4.36
175	2.33	0.45	168	0.030	0.034	0.065	5.27

Vita

Daniel Pfeffer was born in Mount Juliet, TN on May 5, 1983. He went to high school at Mt. Juliet High School where he found a passion for science. Then he went on to the University of Tennessee in Knoxville to pursue a Bachelor's Degree in Aerospace Engineering. After graduating with his Bachelor's Degree he got an opportunity to pursue his other passion and represent the U.S. in the 2006 Karatedo World Cup in Tokyo, Japan. Then he went back to school to receive his Master of Science degree in Aerospace Engineering at the University of Tennessee in May 2007. He will be going on to work in the wonderful world of engineering.